PSS®E composite load and distributed PV model updates

June 2024

CMLD and DER model updates

An addendum to the 'PSSE models for load and distributed PV in the NEM' report released 25/11/2022

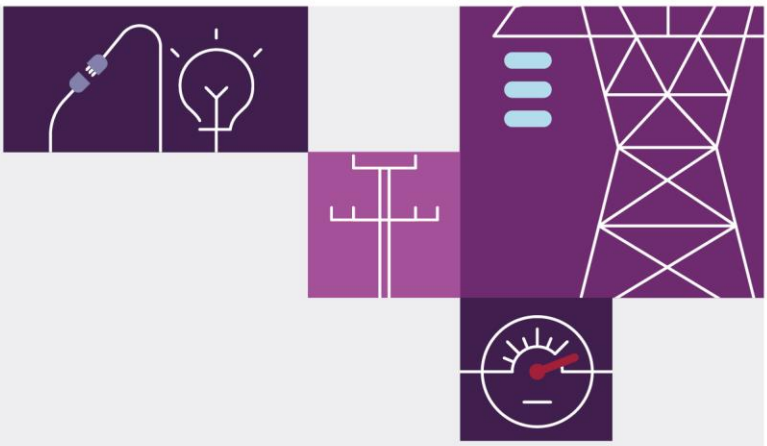

Important notice

Purpose

This report provides information on improvements and further validation of power system models for distributed PV and composite load in PSS®E. It builds on AEMO's previous report[1] which outlined the development of the first release of these models.

AEMO requires accurate power system models for distributed PV (DPV) and load to fulfil responsibilities under the National Electricity Rules to ensure the power system is operated within the limits of the technical envelope (NER 4.3.1(f)), and to have the necessary tools to maintain power system security (NER 4.3.1(a)). AEMO has also provided the models to Network Service Providers, to use at their discretion when developing limit advice.

This report is based on information available to AEMO up to June 2024 unless otherwise indicated.

Disclaimer

AEMO has made reasonable efforts to ensure the quality of the information in this report but cannot guarantee that information, forecasts and assumptions are accurate, complete or appropriate for your circumstances. Any views expressed in this report are those of AEMO unless otherwise stated, and may be based on information given to AEMO by other persons. This report or the information in it may be subsequently updated or amended. This document does not constitute legal, business engineering or technical advice, and should not be relied on as a substitute for obtaining detailed advice about the National Electricity Law, the National Electricity Rules, or any other applicable laws, procedures or policies. Accordingly, to the maximum extent permitted by law, AEMO and its officers, employees and consultants involved in the preparation of this report:

- make no representation or warranty, express or implied, as to the currency, accuracy, reliability or completeness of the information in this report; and
- are not liable (whether by reason of negligence or otherwise) for any statements or representations in this document, or any omissions from it, or for any use or reliance on the information in it.

Copyright

[1] AEMO (November 2022) PSS®E models for load and distributed PV in the NEM, https://aemo.com.au/-/media/files/initiatives/der/2022/psse-models-for-load-and-distributed-pv-in-the-nem.pdf?la=en

AEMO acknowledges the Traditional Owners of country throughout Australia and recognises their continuing connection to land, waters and culture. We pay respect to Elders past and present.

Executive summary

In November 2022, AEMO released new models that aimed to better represent the complex behaviours of composite load and distributed PV (DPV) in power system studies[2]. The models are referred to as CMLD (representing composite load) and DERAEMO1 (representing distributed PV).

Since the release of the version 1 models, there has been an increased focus on the transient behaviours of the models, assessing their suitability for application in calculating transient stability limits. This has led to a number of model refinements, which are summarised in this report.

Three areas of update are recommended for the CMLD model parameters:

- **Decrease Motor D composition parameters** – Motor D is a specially developed performance model intended to represent single-phase (1P) compressors of residential air-conditioning loads. In the version 1 model, a proportion of load associated with motor driven refrigerators and freezers was also included in the Motor D component. New laboratory testing results have indicated that fridges and freezers do not appear to demonstrate the stalling behaviour evident from motor driven air conditioners, so the load associated with these devices is better represented in the Motor A category. This reduces the proportion of regional load in the Motor D category from ~1 - 10% in the version 1 model, to 0.2 – 0.4% in the version 2 model (annual average). In peak summer periods (highest 1% of underlying demand), the Motor D composition is estimated to reach a maximum of ~2.5 – 3.2% of load.
- **Update Motor D performance parameters** – The laboratory testing of Motor D loads provides an opportunity to fine tune the performance of the Motor D model to better represent observed device behaviours. EPRI has also released updated recommended default parameters, which were adopted where better local data was not available.
- **Simplify CMLD composition parameters** – The version 1 CMLD model utilised varying composition parameters which adjusted the proportions of load in each category by season, date and time of day. Model testing has indicated that this degree of variability in load composition does not lead to important differences in modelling outcomes, except for peak summer conditions where modelling indicates the VNI transient stability export limit used for validation studies[3] can be around 80 MW lower. It is therefore proposed for version 2 to apply just a single set of load composition parameters in all periods, based on the annual average. The composition parameters for peak summer conditions have also been provided and the user may use their discretion to apply these parameters instead if appropriate.

The impacts of the CMLD model were tested on certain VNI transient stability export limits[3], to give a preliminary indication of the influence of the models and these changes. It was found that the version 2 CMLD parameters, compared with the older ZIP model, does appear to have a meaningful impact on these VNI limits. Further analysis is required to fully investigate the impacts of these updated models on transmission network stability

[2] AEMO (November 2022) PSS®E models for load and distributed PV in the NEM, https://aemo.com.au/-/media/files/initiatives/der/2022/psse-models-for-load-and-distributed-pv-in-the-nem.pdf?la=en

[3] V::N_NIL_V and V::N_NIL_O, Victorian transient stability export limits on the VIC to NSW interconnectors for the two phase to ground fault and trip of Hazelwood – South Morang 500kV line.

limits. This suggests transmission network service providers should investigate the impacts of these models on their limit advice.

These updates were tested to confirm they do not significantly affect the representation of load and DPV shake-off behaviours (disconnection of DPV and load in response to a fault), which were carefully calibrated in the version 1 parameter sets. The tests indicate that the shake-off estimates from the model remain appropriate, and no re-calibration of the shake-off parameters is required at this time.

The transient behaviours of the CMLD and DERAEMO1 models were also compared with measured observations of load behaviours in response to deep faults at certain locations in the Victorian network (at the limited locations where high speed measurement is available at radial load locations). It was found that the CMLD and DERAEMO1 models produce a considerable improvement in the representation of reactive power dynamics in the transient period during and immediately following a fault, and somewhat of an improvement in the active power dynamics (compared with the earlier ZIP load model). Further improvements in the calibration of load and DER models will rely on increasing the availability of high speed measurements at radial load locations. This means that model validation should be better supported in future by the rollout of phasor measurement units (PMUs) across the NEM.

From application of the models to inertia studies, it has been identified that in response to a network fault, the DERAEMO1 model active power recovers approximately 80 ms slower than the CMLD load model, which can lead to a short duration deficit in active power that impacts system frequency in low inertia conditions. Bench testing data and review of the model parameters suggest that the delayed recovery of the DERAEMO1 model is reasonable, and reflective of real measurement and processing delays.

AEMO recommends that stakeholders adopt these updated version 2 parameters in any future studies that utilise these models. The CMLD and DERAEMO1 models provide important improvements in load and DPV representation in power system studies compared with the earlier ZIP load models, but also have many remaining limitations, and should be applied with discretion and only when appropriate. AEMO will continue to work with TNSPs on improvements to these models.

Contents

Executive summary		3
1	Introduction	9
2	CMLD Parameter Updates	10
2.1	Summary of the CMLD model	10
2.2	Motor D investigation	11
2.3	Simplifying CMLD composition parameters	18
2.4	Implications of the proposed CMLD updates for stability limits	20
3	Model validation	22
3.1	Shake-off behaviours	22
3.2	Transient behaviours (SLIB validations)	23
4	Active power recovery rates	29
5	Next Steps	33
A1.	DERAEMO1 summary	34
A1.1	Under-voltage response	34
A1.2	Over-voltage response	36
A1.3	Reactive Power-Voltage response	37
A1.4	Under-frequency response	37
A1.5	Over-frequency response	38
A1.6	Response to Rate of Change of Frequency (RoCoF)	38
A2.	DERAEMO1 parameters	40
A2.1	Voltage control parameters	40
A2.2	Voltage tripping parameters	40
A2.3	Frequency control parameters	41
A2.4	Frequency tripping parameters	42
A2.5	RoCoF tripping parameters	44
A3.	CMLD summary	45
A3.1	CMLD overview	45
A3.2	Under-voltage response of CMLD	45
A3.3	Over-voltage response of CMLD	46
A3.4	Frequency response of CMLD	46
A4.	CMLD Parameters (version 2)	48
A4.1	CMLD composition parameters	48
A4.2	CMLD feeder parameters	49
A4.3	CMLD performance parameters	50

A5. CMLD version 1 and version 2 comparison 54
A6. Transient behaviour validation testing 57
A6.1 25/07/2022 57
A6.2 18/01/2018 58
A6.3 31/01/2020 62
A6.4 8/03/2018 66
A6.5 18/02/2019 68
A7. Motor D composition estimates 70
A7.1 Estimating the number of residential AC units operating 70
A7.2 Estimating power consumption per unit 70

Tables

Table 1 UoW findings for voltage sag tests 12
Table 2 Total Motor D proportions by region and season 15
Table 3 Summary of proposed Motor D performance parameter changes 16
Table 4 Version 1 CMLD composition parameters for general end-use-load 18
Table 5 Limits used for testing of the influence of CMLD model parameters 18
Table 6 Annual average composition fractions for general end-use loads 20
Table 7 Validation event summary – Minimum voltages recorded (pu) 23
Table 8 Legend for tables below 26
Table 9 Active power - Transient 27
Table 10 Reactive power - Transient 27
Table 11 Active power – Steady State 27
Table 12 Reactive power – Steady State 28
Table 13 Factors in DERAEMO1 which influence active power recovery post fault 30
Table 14 vrfrac block parameters – under-voltage behaviour 35
Table 15 vrfrac block parameters – over-voltage behaviour 36
Table 16 Under-frequency tripping stages 37
Table 17 Over-frequency tripping stages 38
Table 18 RoCoF trip stages 39
Table 19 Voltage Control Parameters in the DERAEMO1 model (identical for all regions) 40
Table 20 Voltage tripping parameters in the DERAEMO1 model (identical for all regions) 40
Table 21 Voltage tripping parameters in the DERAEMO1 model that vary between regions 40
Table 22 Frequency control parameters in the DERAEMO1 model (identical for all regions) 41
Table 23 Frequency control parameters in the DERAEMO1 model that vary between regions 41

Table 24	Frequency tripping parameters in the DERAEMO1 model (identical for all regions)	42
Table 25	Frequency tripping parameters in the DERAEMO1 model that vary between regions	43
Table 26	Frequency tripping parameters in the DERAEMO1 model (identical for all regions)	44
Table 27	Frequency tripping parameters in the DERAEMO1 model that vary between regions	44
Table 28	Load composition parameters for Auxiliary and Large Industrial Loads	48
Table 29	Load composition parameters for general end-use-load – Annual average	48
Table 30	Load composition parameters for general end-use-load – Peak Summer	49
Table 31	Feeder configuration parameters (depending on load type)	49
Table 32	Common feeder parameters	49
Table 33	Power electronics performance parameters	50
Table 34	Static load performance parameters	50
Table 35	Motor A performance parameters	50
Table 36	Motor B performance parameters	51
Table 37	Motor C performance parameters	51
Table 38	Motor D performance parameters	52

Figures

Figure 1	The composite load model (CMLD) structure	10
Figure 2	Example air conditioner bench test: voltage sag (0.2pu for 120ms)	12
Figure 3	Active Power: Comparison of aggregated ACs and aggregated fridge/freezers (0.4pu for 80ms)	13
Figure 4	Reactive Power: Comparison of aggregated ACs and aggregated fridge/freezers (0.4pu for 80ms)	14
Figure 5	Motor D model performance – comparison to measured behaviour (0.2pu for 120ms)	17
Figure 6	Comparison of limits with annual average load composition versus seasonal composition	19
Figure 7	Voltage disturbances: Model performance for load/DPV shake-off – Version 2 parameters	22
Figure 8	Network locations with high speed monitoring of radial loads	24
Figure 9	Cranbourne network (CBTS) used for SLIB validation studies (18 January 2018)	25
Figure 10	18/01/2018 – Cranbourne (CBTS) – Typical example	26
Figure 11	Example of active power recovery rates post fault	30
Figure 12	DER model – Current/Output control	31
Figure 13	Example inverter bench test result – 0.2pu sag for 80ms	32
Figure 14	vrfrac block	35
Figure 15	CMLD version 1 vs CMLD version 2 during the modelled event on 8/3/18	54
Figure 16	CMLD version 1 vs CMLD version 2 during Hazelwood-South Morang 2PH-G fault	55

Figure 17 CMLD version 1 vs CMLD version 2 during Hazelwood-South Morang1PH-G fault: impact to Vic-NSW flows 56
Figure 18 Red Cliffs (RCTS) 58
Figure 19 Brooklyn (BLTS) 59
Figure 20 Cranbourne (CBTS) 60
Figure 21 Rowville (ROTS) / Springvale (SVTS) 61
Figure 22 Templestowe (TSTS) 62
Figure 23 Brooklyn (BLTS) 63
Figure 24 Cranbourne (CBTS) 64
Figure 25 Rowville (ROTS) / Springvale (SVTS) 65
Figure 26 Templestowe (TSTS) 66
Figure 27 Rowville (ROTS) / Springvale (SVTS) 67
Figure 28 Templestowe (TSTS) 68
Figure 29 Rowville (ROTS) / Springvale (SVTS) 69

1 Introduction

AEMO and network service providers (NSPs) use power system models to assess power system performance under different conditions. The results from these studies inform operational and planning decisions, allowing AEMO to fulfill its responsibilities to maintain a secure power system.

In November 2022, AEMO released new models that aimed to better represent the complex behaviours of composite load and distributed PV (DPV) in power system studies[4]. The models are referred to as CMLD (representing composite load) and DERAEMO1 (representing DPV). A summary of the functionality of the CMLD and DERAEMO1 models is provided in Appendix A1 and Appendix A3 of this report.

In the development of the initial versions of these models, there was a significant focus on calibrating "shake-off" behaviours (disconnection of load and DPV in response to a transmission network fault). The version 1 models provided a considerably improved representation of shake-off (compared with the earlier ZIP load model), and have been made available to NSPs to capture these behaviours in their limits assessments and other studies where appropriate. Many areas for further improvement of the models were also identified.

Since the release of the version 1 models, there has been an increased focus on the transient behaviours of the models, assessing their suitability for application in calculating transient stability limits. This has led to a number of model refinements, which are summarised in this report.

This report covers:

- Proposed refinements to the CMLD model parameters (Section 2), including:
  - Updates to composition fractions
  - Updates to "Motor D" model parameters based on laboratory testing results
  - Reducing the complexity of the CMLD model
- Model validation (Section 3), including:
  - Confirming that with these parameter updates the models remain appropriate for representing shake-off behaviours
  - Validation of transient behaviours against radial load measurements in Single Load Infinite Bus (SLIB) studies
- Assessment of active power recovery rates, and implications for studies (Section 4)

This report is prepared for transparency with stakeholders on this ongoing work program, as these models may be progressively applied by AEMO and TNSPs for assessment of power system limits and application in other operational and planning processes. Many further areas of improvement remain, and ongoing work will continue to be communicated to stakeholders as it progresses.

[4] AEMO (November 2022) PSS®E models for load and distributed PV in the NEM, https://aemo.com.au/-/media/files/initiatives/der/2022/psse-models-for-load-and-distributed-pv-in-the-nem.pdf?la=en

2 CMLD Parameter Updates

2.1 Summary of the CMLD model

The composite load model applied in these studies is shown in Figure 1. It consists of six load components at the end of a feeder equivalent circuit, which is represented by a series impedance and shunt compensation. It is intended to emulate various load components' aggregate behaviour. It includes 3 three-phase (3P) induction motor models (Motor A, B and C), a single-phase (1P) capacitor-start motor performance model (Motor D), static load components (constant current and constant impedance), and a power electronic load model (constant active and reactive power).

Figure 1 The composite load model (CMLD) structure

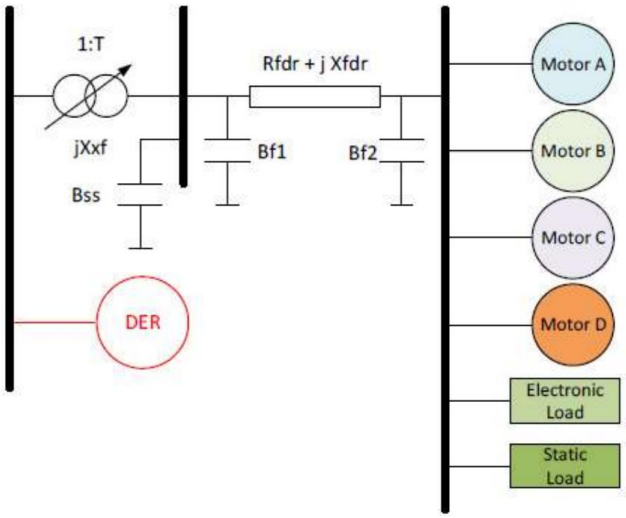

Further background on the model and development of suitable parameters for each component is provided in AEMO's original report[5]. The full set of recommended parameters for the CMLD model is summarised in Appendix A4.

2.1.1 Motor D

Motor D is a specially developed performance model intended to represent single-phase (1P) compressors of residential air-conditioning loads. A constant torque load characteristic and minimal inertia make these motors prone to stall. This motor type is also common in 1P residential and light commercial refrigerator compressor motors in Australia. The typical rating is between 2 to 4 kW.

The Motor D model is of particular importance in the USA, where a large proportion of load (up to 40%) can be supplied by Motor D type loads at certain times, and this can lead to observations of Fault Induced Delayed

[5] AEMO (November 2022) PSS®E models for load and distributed PV in the NEM, https://aemo.com.au/-/media/files/initiatives/der/2022/psse-models-for-load-and-distributed-pv-in-the-nem.pdf?la=en

Voltage Recovery (FIDVR), which refers to delay in the recovery of voltage to its nominal value following the normal clearing of a fault[6].

In the initial development of the CMLD parameters, AEMO was aware that the proportion of load supplied by Motor D type loads is much lower in Australia due to a higher prevalence of inverter-driven residential air conditioning units. AEMO commissioned several studies to estimate the proportion of load supplied by Motor D in Australia[7], and also to conduct some stall test measurements for refrigerators[8] (which form a substantial proportion of the Motor D load in Australia). These investigations suggested that refrigerator and air conditioning load combined (which was originally categorised as Motor D in Version 1 of the CMLD parameters) typically supplies 1-10% of regional load (depending on the region and time period, see Table 4).

Even at these low levels, subsequent studies indicated that the Motor D component was having a significant influence on power system stability limits in the NEM (refer to Section 2.4). This initiated further investigation to confirm if these effects were valid and appropriate, as summarised below.

2.2 Motor D investigation

2.2.1 Bench Testing

AEMO commissioned University of Wollongong (UoW) to perform a series of voltage sag tests on a variety of Motor D type loads, and test their responses[9]. The UoW test facilities provided much higher resolution measurements than those originally conducted for AEMO by EES[10]. The testing methodology in the EES study was largely targeted at finding the point at which the unit disconnects or stalls, and involved extended duration voltage sags (in the order of tens of seconds). The UoW testing provides a better indication of Motor D device behaviours in response to short duration deep voltage sags, more representative of network conditions experienced in response to credible power system faults.

UoW procured 6 air conditioners (ACs) and 7 fridges/freezers, including sourcing a selection of older models from second hand markets to be more representative of the likely load composition at present.

Figure 2 shows an example of a 120 ms duration 0.2 p.u. voltage sag test on an air-conditioner that exhibits stalling behaviour. When the voltage sag occurs, there is insufficient power available to keep the motor operating. The device stalls, increasing the current supplied significantly. When the voltage sag is removed, the current on the stalled device remains high. This results in the active and reactive power drawn by the air conditioner increasing significantly for approximately 6 seconds, at which point the unit disconnects on thermal protection.

[6] IEEE (August 2019) Fault Induced Delayed Voltage Recovery (FIDVR): Modelling and Guidelines, at https://ieeexplore.ieee.org/document/8973440

[7] Energy Efficient Strategies (31 July 2020) Single Phase Induction Motor Loads on the NEM from Refrigeration and Air Conditioners, https://aemo.com.au/-/media/files/initiatives/der/2020/2020-08-05-ees-ac-load-composition.pdf?la=en

[8] Energy Efficient Strategies (26 June 2020) Results of low voltage stall measurements on single phase induction motors and inverter systems, https://aemo.com.au/-/media/files/initiatives/der/2020/2020-08-05-ees-results-of-stall-measurements-on-motor-d-and-inverter-systems.pdf?la=en

[9] University of Wollongong (June 2024) Composite Load Model Motor D Testing, at https://aemo.com.au/initiatives/major-programs/nem-distributed-energy-resources-der-program/operations/power-system-model-development

[10] Energy Efficient Strategies (26 June 2020) Results of low voltage stall measurements on single phase induction motors and inverter systems, https://aemo.com.au/-/media/files/initiatives/der/2020/2020-08-05-ees-results-of-stall-measurements-on-motor-d-and-inverter-systems.pdf?la=en

Figure 2 Example air conditioner bench test: voltage sag (0.2pu for 120ms)

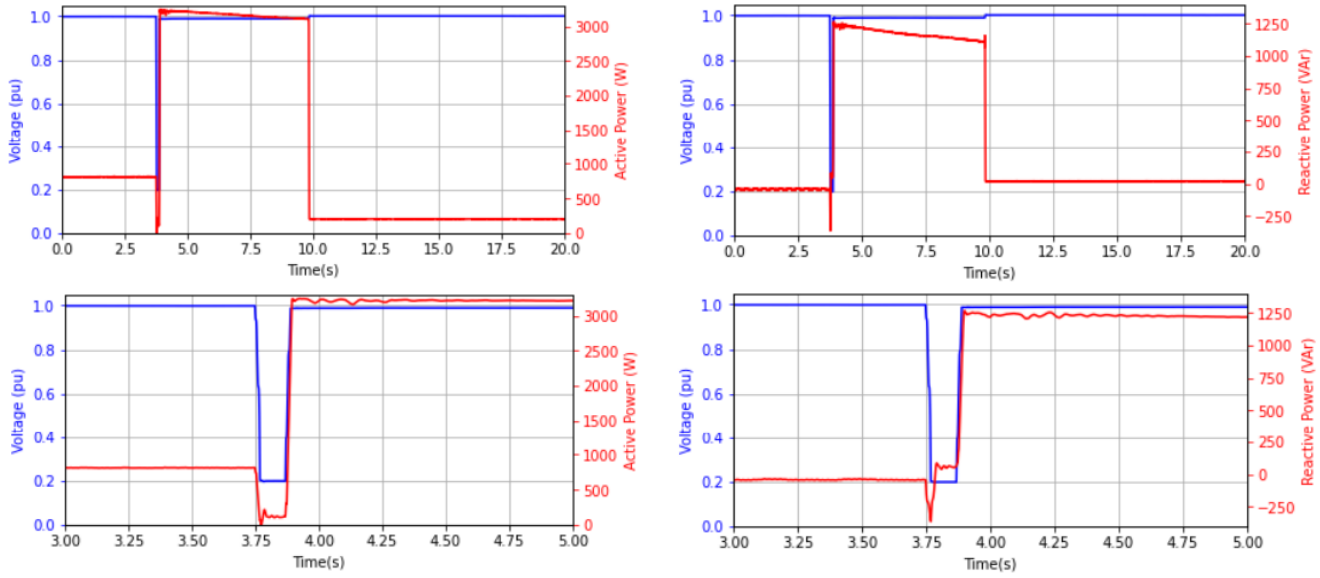

Top 2 panels: response over a 20 second period. Bottom 2 panels: response over a 2 second period.

Table 1 summarises observations for all the devices tested. The results indicate that the air conditioners generally behave in a similar manner to those tested in the USA, demonstrating stalling behaviour for voltage sags below ~0.5pu. However, the refrigerators and freezers tested appear to be less prone to stalling behaviour.

Table 1 UoW findings for voltage sag tests[11]

Load type	Test under which device begins to stall	Test under which device begins to disconnect
AC 1	0.5 pu for 80 ms	0.2 pu for 400 ms
AC 2	0.6 pu for 80 ms	0.2 pu for 400 ms
AC 3	0.6 pu for 80 ms	0.5 pu for 80 ms
AC 4	0.6 pu for 80 ms	0.6 pu for 80 ms
AC 5	0.6 pu for 120ms	0.5 pu for 80 ms
AC 6	0.5 pu for 80 ms	0.3 pu for 120 ms
Fridge 1 (newer fridge)	0.2 pu for 120ms	0.2 pu for 400 ms
Fridge 2 (old fridge)	0.2 pu for 120 ms	0.2 pu for 120 ms
Fridge 3 (newer fridge)	0.2 pu for 400 ms	0.2 pu for 400 ms
Fridge 4 (old fridge)	No stall	No disconnect
Fridge 5 (old fridge)	0.2 pu for 400 ms	0.2 pu for 400 ms
Freezer 1 (old freezer)	0.2 pu for 400 ms	0.2 pu for 400 ms
Freezer 2 (new freezer)	0.4 pu for 80 ms	0.4 pu for 120 ms

This suggests that refrigerators and freezers should not be included in the Motor D category in the model. Based on these new test results, AEMO proposes that the load associated with these devices should be included in the

[11] University of Wollongong (June 2024) Composite Load Model Motor D Testing, at https://aemo.com.au/initiatives/major-programs/nem-distributed-energy-resources-der-program/operations/power-system-model-development

Motor A category instead (intended to represent refrigeration systems, albeit three phase systems). In the test results, these fridges and freezers demonstrate a significant in-rush current (and subsequently increased active and reactive power) for a short duration immediately following the fault as the motor returns to nominal speed. This behaviour is best represented by the Motor A component of the CMLD model, as Motor A exhibits the highest in-rush current.

The aggregated AC and fridge/freezer responses for a 0.4 pu voltage sag, 80 ms duration, are shown in Figure 3 and Figure 4.

Figure 3 Active Power: Comparison of aggregated ACs and aggregated fridge/freezers (0.4pu for 80ms)

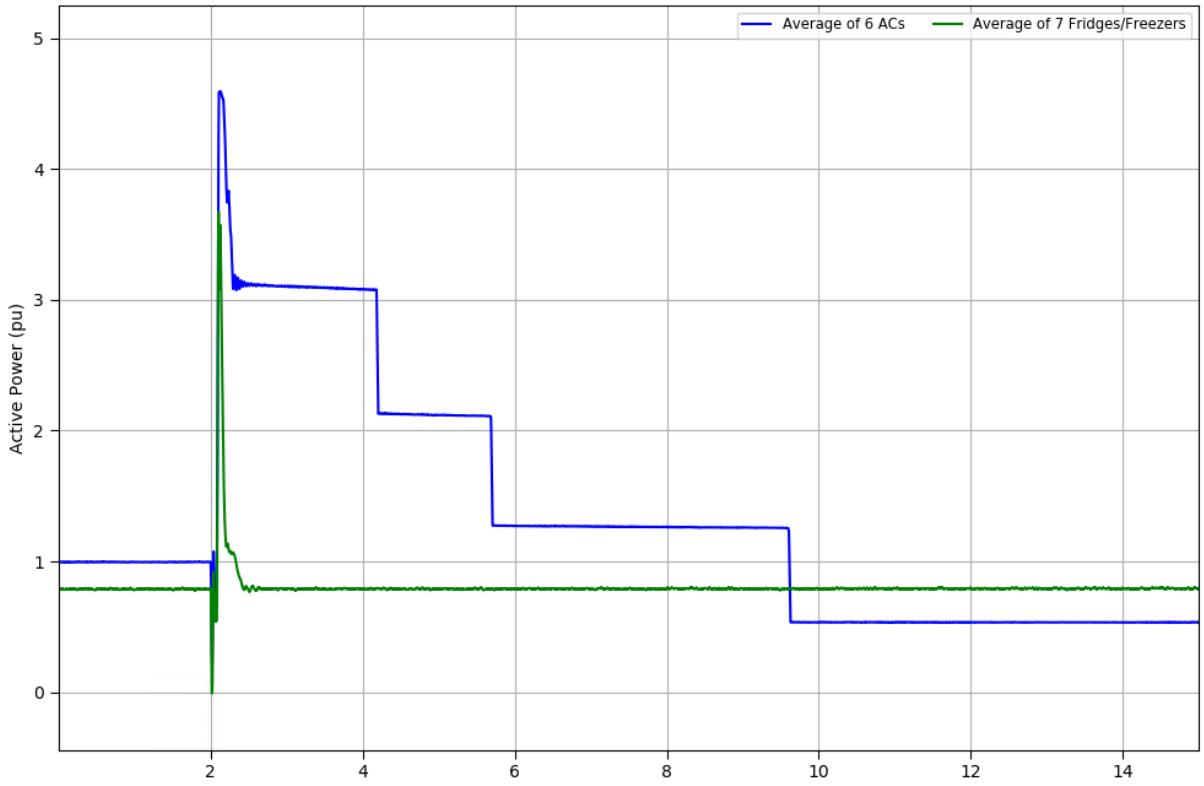

Figure 4 Reactive Power: Comparison of aggregated ACs and aggregated fridge/freezers (0.4pu for 80ms)

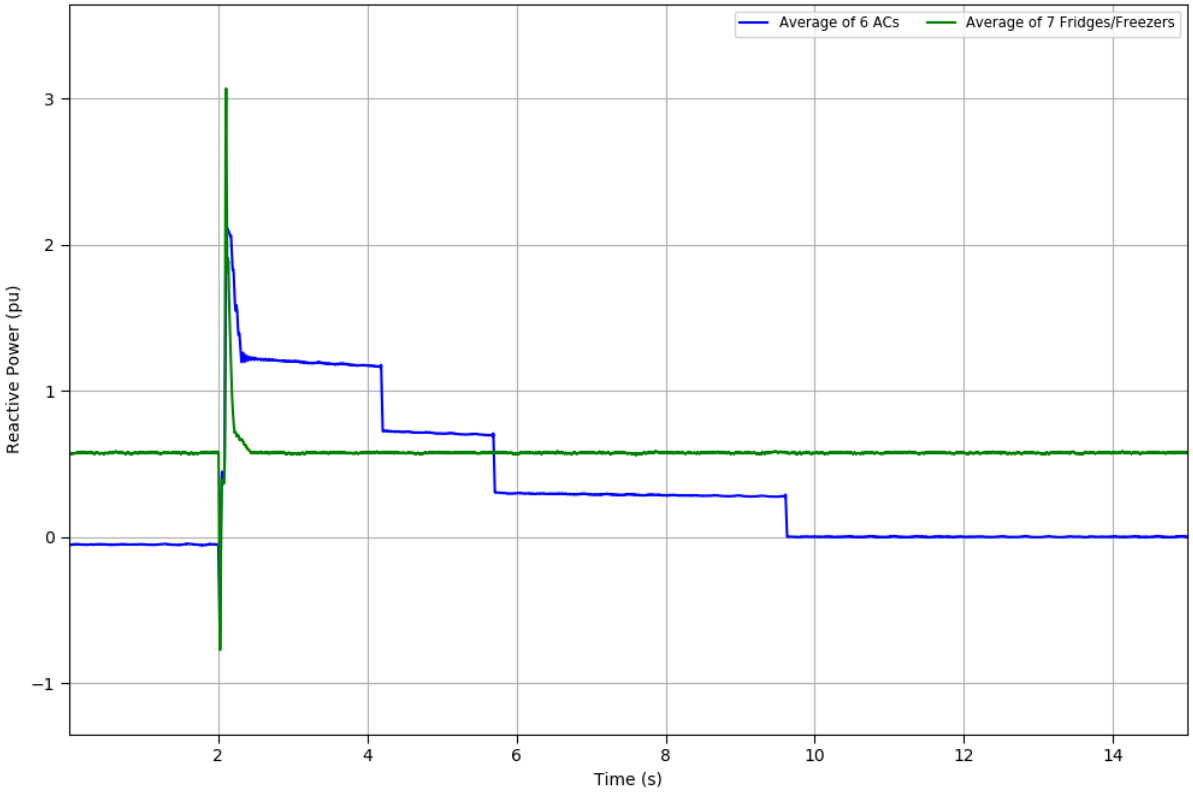

Proposed update 1: Move refrigerators and freezers from Motor D to Motor A

Based on new laboratory testing results, it is proposed that load associated with refrigerators and freezers should be moved from Motor D to Motor A, since these types of devices do not appear to demonstrate stalling behaviour consistent with the Motor D model.

The re-calibration of the composition parameters to reflect this change is outlined in Section 2.2.2.

Proposed update 2: Fine-tune Motor D parameters to better represent tested devices

Based on these new laboratory testing results, AEMO has fine-tuned the Motor D parameters to better represent the observed device behaviours. The proposed new parameters are summarised in Section 2.2.3

2.2.2 Motor D Composition Factors

AEMO re-calculated the CMLD composition parameters to move load associated with fridges and freezers from Motor D to Motor A. Since the release of the version 1 models, some new datasets have also become available and these were taken into account in this review of the CMLD composition parameters. This included:

- The 2021 Residential Baseline Study for Australia and New Zealand[12] (released in November 2022). This study provides a detailed breakdown of residential load into various appliance types. This gives a significant update since the earlier dataset (released in 2015) used for the version 1 models.
- CSIRO datasets to estimate the correlation between AC load and temperature/season[13].
- Information from the original EES report[14] (developed for AEMO and used for the version 1 models) was also used to estimate the proportion of ACs that are single-phase induction motor driven.

For each NEM region, the proportion of load associated with single-phase induction motor AC loads was calculated for each season[15]. Motor D load in a "peak" load summer interval was also estimated, since there can be a large difference in the total AC load between peak summer load days compared to typical summer days. The total load for each type of interval was calculated by multiplying the estimated number of Motor D appliance units operating by the estimated power consumption per unit (with both factors varying by season).

Table 2 shows the estimated proportions of load in the Motor D category. These are significantly reduced from the previous Motor D composition estimates of 1-10% (used in the version 1 model, see Table 4). Section 2.3 discusses further how these estimated Motor D proportions have been integrated into the version 2 parameter sets.

Table 2 Total Motor D proportions by region and season

Interval	VIC	QLD	NSW	SA
Peak Summer (highest 1% underlying demand)	2.9%	2.5%	3.0%	3.2%
Typical Summer	0.5%	0.6%	0.5%	1.1%
Shoulder	0.1%	0.1%	0.1%	0.1%
Winter	0.0%	0.1%	0.0%	0.4%

2.2.3 Motor D performance parameter updates

Since the version 1 release of the CMLD model in November 2022, EPRI (leading a significant international work program on load/DER models) has made some updates to their recommended default Motor D parameters. This, along with the UoW bench test data, presents an opportunity to refine the Motor D model performance parameters. AEMO's updated parameters adopt EPRI's default Motor D parameters, with some further adjustments to better represent the observed behaviour in the UoW bench-test data.

Table 3 below summarises the recommended changes to the Motor D performance parameters, based on these new information sources. The grey rows outline where AEMO has adopted the updated recommended parameters

[12] Australian Government (11 November 2022) 2021 Residential Baseline Study for Australia and New Zealand for 2000 to 2040, https://www.energyrating.gov.au/industry-information/publications/report-2021-residential-baseline-study-australia-and-new-zealand-2000-2040

[13] M..Goldsworthy, CSIRO, (24 August 2017). "Towards a Residential Air-Conditioner Usage Model for Australia", https://www.mdpi.com/1996-1073/10/9/1256

[14] Energy Efficient Strategies (31 July 2020) Single Phase Induction Motor Loads on the NEM from Refrigeration and Air Conditioners, https://aemo.com.au/-/media/files/initiatives/der/2020/2020-08-05-ees-ac-load-composition.pdf?la=en

[15] Summer (Dec – Feb), Winter (Jul – Aug) & Shoulder (Mar-May and Sept - Nov)

provided by EPRI. The purple rows outline where further adjustments were made so that the Motor D response better aligns with the observed bench test data.

Table 3 Summary of proposed Motor D performance parameter changes[16]

Motor D performance parameters	Description	AEMO version 1 (based on EES testing[17] in 2020)	EPRI latest[18]	AEMO version 2 proposed
Tf	frequency time constant for contactors (s)	0.1	0.05	0.05
compPF	power factor at 1 pu voltage	0.71	0.98	**1.00**
Vstall	stall voltage (pu)	0.49	0.45	**0.6**
Rstall	stall resistance (pu of motor base)	0.143	0.1	**0.17**
Xstall	stall reactance (pu of motor base)	0.143	0.1	**0.07**
Frst	fraction capable of restart after stall	0.1	0.2	**0.55**
Vrst	voltage for restart after stall (pu)	0.95	0.95	**0.9**
Tth	heating time constant (s)	15	10	**16**
Th1t	temperature where tripping begins (pu)	1.98	0.7	0.7
Th2t	temperature where completely tripped (pu)	4.59	1.9	1.9
Fuvr	Fraction with undervoltage relays	0.325	0.1	0.1[19]
Uvtr1	1st undervoltage pick-up (pu)	0.55	0.6	0.6
Ttr1	1st undervoltage trip delay (s)	0.06	0.02	0.02
Uvtr2	2nd undervoltage pick-up (pu)	0.1	0	0

Figure 5 shows the UoW bench testing results, averaged (per unit) across the six AC units tested (in blue). These results were used to further adjust the updated EPRI default parameters which led to the development of the novel version 2 parameters in Table 3. The AC units were each subjected to a 0.2 pu voltage sag for a duration of 120 ms, and the active/reactive power responses of each unit recorded (shown in aggregate in blue in Figure 5).

For comparison, Figure 5 also shows the Motor D model performance in response to an identical voltage sag, with the CMLD Motor D component modelled as a single load infinite bus (SLIB) in PSS®E. Figure 5 compares the Motor D response with the EPRI recommended default parameters (in red), and AEMO's recommended parameters (in green). The AEMO recommended parameters have been tuned to better match the observed UoW bench testing results, adjusting compPF, Vstall, Rstall, Xstall, Frst, Vrst, Tth (as defined in Table 3 above),

[16] A more detailed outline of the impact of these parameters on model response can be found in this report published by the Western Electricity Coordinating Council (WECC): WECC Composite Load Model Specification (April 2021), https://www.wecc.org/Reliability/WECC%20Comp%20Load%20Model%20Specification_final.pdf

[17] Energy Efficient Strategies (26 June 2020) Results of low voltage stall measurements on single phase induction motors and inverter systems, https://aemo.com.au/-/media/files/initiatives/der/2020/2020-08-05-ees-results-of-stall-measurements-on-motor-d-and-inverter-systems.pdf?la=en

[18] EPRI (23 September 2020), Technical Reference on the Composite Load Model, https://www.epri.com/research/products/000000003002019209

[19] During parameter tuning to align with the UoW bench test data, the Fuvr parameter was temporarily set to 0, as no undervoltage relay behaviour was exhibited in the air-conditioner test results.

and otherwise adopting the recommended EPRI default parameters. The AEMO recommended parameters also demonstrate a good match with a less severe voltage sag of 0.4 pu for 80 ms.

Figure 5 Motor D model performance – comparison to measured behaviour (0.2pu for 120ms)

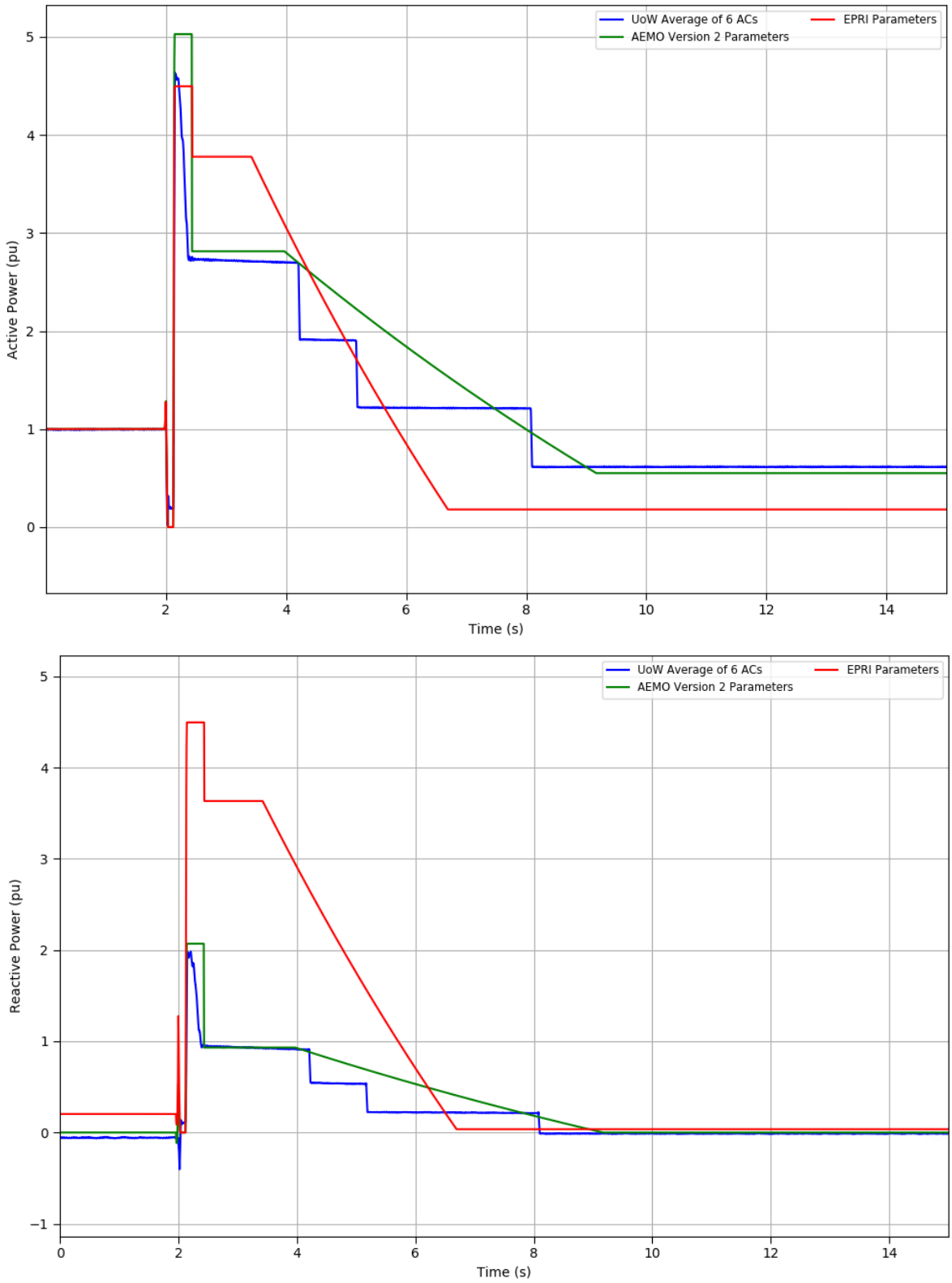

2.3 Simplifying CMLD composition parameters

The version 1 CMLD model had load composition parameters for general end-use load that vary by time of day, season and region. Table 4 summarises the ranges of these parameters, as applied in version 1. As part of this update, AEMO has sought to simplify the application of the model, moving towards a smaller set of representative composition parameters.

Table 4 Version 1 CMLD composition parameters for general end-use-load

	NSW	VIC	QLD	SA	TAS
Motor A	7.1% - 12.4%	6.3% - 10.6%	7.9% - 11.0%	4.1% - 7.6%	8.5% - 11.9%
Motor B	14.5% - 18.1%	15.8% - 20.6%	20.6% - 25.3%	13.4% - 18.2%	22.0% - 25.7%
Motor C	11.8% - 14.2%	10.8% - 14.1%	12.4% - 15.8%	11.2% - 15.3%	20.1% - 24.1%
Motor D	2.7% - 6.2%	3.9% - 9.1%	2.3% - 4.9%	3.9% - 10.1%	1.2% - 2.5%
Power Electronic	30.0% - 36.4%	30.7% - 37.5%	29.0% - 37.3%	33.1% - 44.0%	24.4% - 25.7%
Constant Current	3.5% - 6.2%	3.5% - 6.6%	3.4% - 5.7%	2.8% - 6.1%	4.5% - 5.6%
Constant Impedance	14.6% - 23.3%	12.1% - 18.8%	8.1% - 15.6%	11.1% - 21.2%	8.0% - 15.8%

To test the potential for simplifying the load composition parameters, the variability of the composition parameters was analysed. It was determined that the most significant variability was between seasons, with time of day, and day versus night differences being much less significant than the estimated seasonal variations.

Sets of seasonal composition parameters were developed by averaging the time varying composition dataset within each seasonal period[20]. Due to the significant contribution of Motor D load in the highest peak demand periods, a summer peak composition set was also estimated (based on the highest 1% of underlying load periods in each region).

2.3.1 Testing the influence of seasonal composition parameters

The influence of the variation between the different seasonal composition parameters was tested based on impacts on the VNI export limits summarised in Table 5. These limits manage exports over the VIC-NSW interconnector (VNI), to avoid instability in the case of a two phase to ground fault and trip of the Hazelwood – South Morang 500kV line. The CMLD model was applied to studies to investigate impacts on these limits with various assumptions.

Table 5 Limits used for testing of the influence of CMLD model parameters

Constraint Equation	Description
V::N_NIL_V	Victorian transient stability export limit on the VIC to NSW interconnectors for the two phase to ground fault and trip of Hazelwood – South Morang 500kV line where instability occurs due to VIC generators accelerating away from the generators of all the other regions.
V::N_NIL_O	Victorian transient stability export limit on the VIC to NSW interconnectors for the two phase to ground fault and trip of Hazelwood – South Morang 500kV line where instability occurs due to generators in regions other than Victoria accelerating or decelerating away from the generators of all the other regions.

[20] Summer (Dec – Feb), Winter (Jul – Aug) & Shoulder (Mar-May and Sept - Nov)

The studies involved:

- Extracting a large number of different snapshots of the power system from recent historical periods in different types of operating conditions
- In each snapshot, simulating the two phase to ground fault and trip of Hazelwood – South Morang 500kV line.
- In each snapshot, incrementally increasing exports on VNI until instability is observed. The limit in each snapshot period is the last stable level of VNI flows modelled.

These studies would then typically be used to determine a limit equation by developing a suitable regression against relevant system parameters.

The results of these tests are shown in Figure 6. The updated version 2 Motor D performance parameters have been applied for these tests (as summarised in Section 2.2.3) as well as the DERAEMO1 model to represent DPV generation. These studies suggest that all the different seasonal composition fractions produce very similar limit outcomes to the annual average composition fractions, besides the peak summer composition fractions where the limit is ~80 MW lower. This suggests that a single set of composition parameters could be applied and adequately represent the load composition variability. AEMO intends to use the annual average of composition fractions across all study cases. For peak summer conditions (defined as the highest 1% of underlying demand periods), the user may use their discretion to apply these composition fractions (provided in Appendix A4.1.2) instead if appropriate.

Figure 6 Comparison of limits with annual average load composition versus seasonal composition

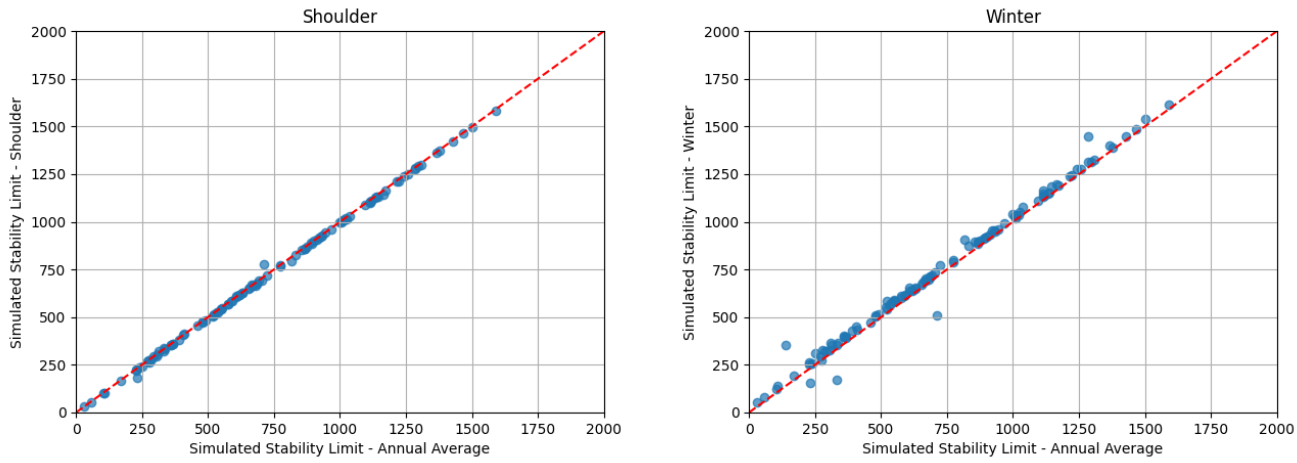

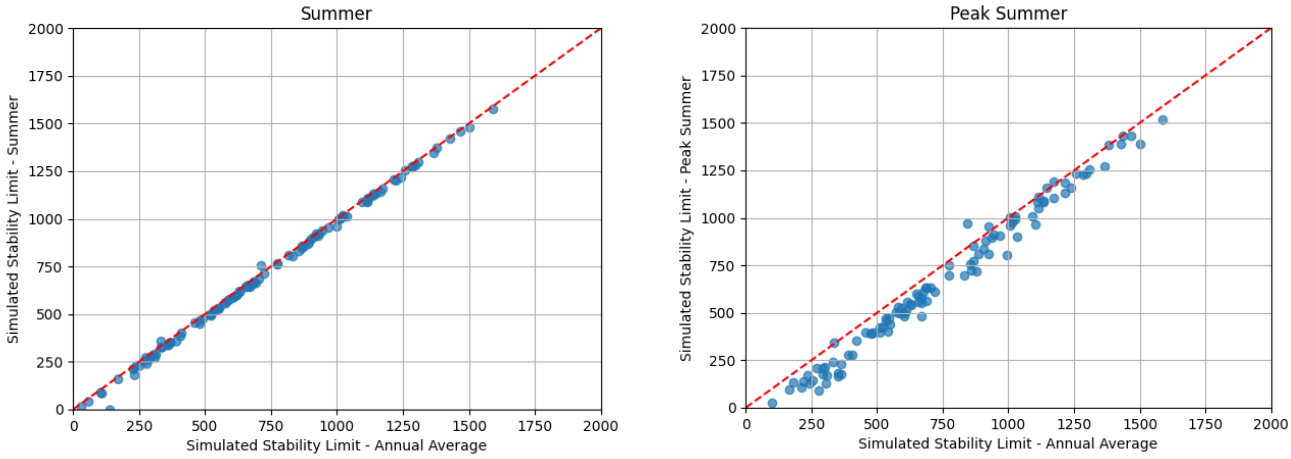

The final revised load fractions (recommended for application in version 2 of the CMLD model) are presented in Table 6. This composition estimate includes the reallocation of refrigeration load from Motor D to Motor A, as described in Section 2.2.2.

Table 6 Annual average composition fractions for general end-use loads

	Motor A	Motor B	Motor C	Motor D	Power Electronic	Constant Current	Constant Impedance	Load Relief*
VIC	15.3%	18.7%	12.4%	0.2%	35.0%	4.6%	13.9%	0.60%
NSW	15.2%	16.6%	12.9%	0.2%	33.7%	4.5%	16.9%	0.56%
QLD	13.3%	23.7%	13.9%	0.2%	34.7%	4.1%	10.0%	0.73%
SA	12.5%	16.5%	12.8%	0.4%	40.1%	3.8%	13.9%	0.56%

* Load relief estimates are provided as an indicative estimate. This is not a parameter in the model, but rather a bottom-up calculation based on the amount of load relief inherently provided by each CMLD load component. Load relief was calculated in a SLIB environment. The frequency of the infinite machine was ramped down and the change in load from each motor type was recorded and then used to calculate the load relief per motor type. Based on the composition fractions the load relief for each region was calculated. Refer to AEMO (June 2023) Review of NEM Load Relief, available at: https://aemo.com.au/-/media/files/initiatives/der/2023/2023-05-31-load-relief-fact-sheet-update.pdf?la=en

Proposed update 3: Simplification of composition parameters

The CMLD composition parameters can be simplified to a single set, based on the annual average composition.

2.4 Implications of the proposed CMLD updates for stability limits

2.4.1 CMLD model

The impacts of the CMLD model were tested on certain VNI transient stability export limits (see Table 5), to give a preliminary indication of the influence of the models and these changes. It was found that the overall impact of the version 2 CMLD parameters, compared with the older ZIP model, does have a meaningful impact on these VNI limits. The version 2 CMLD parameters also impacts the limit differently to the CMLD version 1 parameters. This is related to both the smaller estimated fraction of Motor D in the updated composition fractions, resulting in less

motor stalling, as well as the updated Motor D performance parameters (which reduce the impact of Motor D stalling). This suggests transmission network service providers should investigate the impacts of the version 2 CMLD model on their limit advice.

2.4.2 DERAEMO1 model

It was found the VNI transient stability export limits used for these validation studies (see Table 5) were relatively unaffected by the dynamics of the DERAEMO1 model. However, it is important that if the CMLD model is applied in studies, it is correctly used with the DERAEMO1 model if distributed PV generation is present; the models have been designed and validated to be used together. For example, if the DERAEMO1 model is not applied and CMLD is only used to represent net (operational) demand instead of the full amount of underlying demand that is actually present (offset by generation from DERAEMO1), it will likely understate the impact of the CMLD model on the case.

It's likely that other limits will be more affected by the dynamic behaviour of the DERAEMO1 model itself, however this has not been explored for the purpose of this report.

There are no proposed changes to the DERAEMO1 model behaviour for this release (see Appendix A2). The DERAEMO1 parameters used in VNI export transient stability limit studies outlined in this report have been included in Appendix A2. These are the same parameters that have been published with this release of the model. As the DERAEMO1 parameters evolve over time these updates will be released through AMP.

3 Model validation

3.1 Shake-off behaviours

In the original model validation report[21], 12 voltage disturbances were used to tune the original CMLD and DER model parameters to represent observed DPV and load shake-off behaviours. The version 2 model parameters were applied to confirm that these new parameters do not significantly affect the representation of shake-off, as shown in Figure 7. Shake-off was found to be minimally affected by the update to the version 2 parameters, indicating that no recalibration of these parameters is required at this time.

In Figure 7, blue bars indicate the load change predicted by the CMLD model, yellow bars indicate the DPV change predicted by the DPV model, and the red bars indicate the total net contingency size predicted by both models combined. For night events where there is no DPV generation, the yellow and red bars are zero. The target values were estimated based on actual data collected during each event and are indicated with dots, with error bars indicating the uncertainty in the actuals estimates.

Figure 7 Voltage disturbances: Model performance for load/DPV shake-off – Version 2 parameters

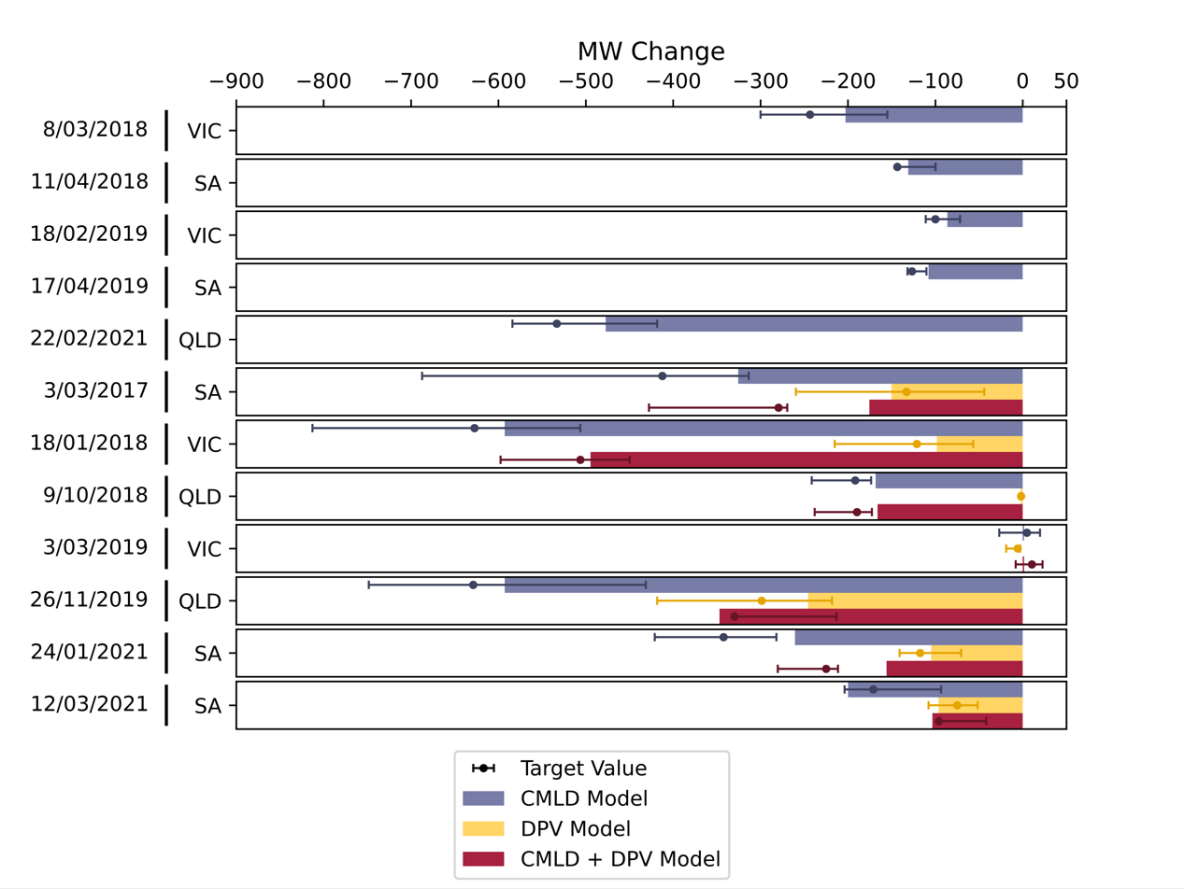

[21] AEMO (November 2022) PSS®E models for load and distributed PV in the NEM, https://aemo.com.au/-/media/files/initiatives/der/2022/psse-models-for-load-and-distributed-pv-in-the-nem.pdf?la=en

Validation of shake-off behaviours

The version 2 updates have minimal impact on the CMLD and DERAEMO1 model load and DPV shake-off behaviours.

3.2 Transient behaviours (SLIB validations)

3.2.1 High speed measurements at radial load locations

To assess the transient behaviours of the CMLD and DERAEMO1 models, AEMO identified locations in the network where there are high speed (~20ms resolution) measurements available at locations with radial loads (not meshed network). The deepest fault events recorded at these locations in recent history were identified. Deep faults at radial load locations provide the best indication of active and reactive power responses of the load itself, without the complicating influences of other nearby generators and network components in a meshed network. At present, there are minimal locations in the NEM with high speed monitoring at radial loads, and all the locations available at present are in the Victorian network only. This represents a significant limitation on the ability to validate and improve load models, and should be addressed in future with an expansion of high speed monitoring capability at a broad selection of radial load sites across all NEM regions.

A summary of the relevant radial load locations and identified events is shown in Table 7. Figure 8 shows a map of the relevant network locations. It is noted that none of these events represent a voltage sag deep enough to lead to Motor D stalling behaviour (which bench testing summarised in Section 2.2.1 indicates occurs for voltage sags below ~0.5pu). This means they have limited ability to validate the Motor D stalling behaviour representation discussed earlier in this report. However, these studies provide a useful validation of the transient behaviour of the CMLD model components in response to milder faults.

Table 7 Validation event summary – Minimum voltages recorded (pu)

Event date	Brooklyn (BLTS)	Cranbourne (CBTS)	Red Cliffs (RCTS)	Rowville (ROTS) / Springvale (SVTS)	Templestowe (TSTS)
25/07/2022	NA	NA	0.63 pu	NA	NA
18/01/2018	0.82 pu	0.64 pu	NA	0.68 pu	0.70 pu
31/01/2020	0.74 pu	0.76 pu	NA	0.76 pu	0.77 pu
8/03/2018	NA	NA	NA	0.75 pu	0.77 pu
18/02/2019	NA	NA	NA	0.84 pu	NA

Figure 8 Network locations with high speed monitoring of radial loads

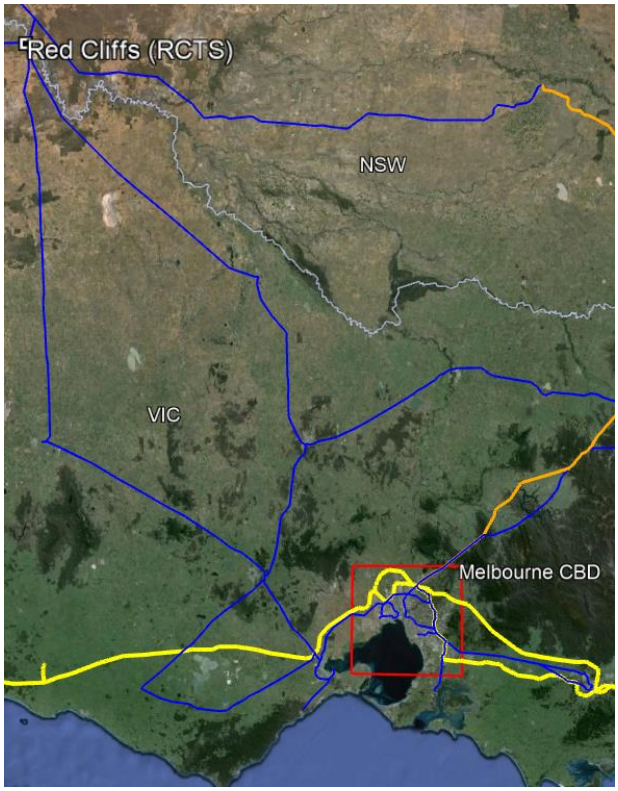

Location: Victoria

Yellow: 500 kV network
Orange: 330 kV network
Blue: 220 kV network

Location: Melbourne CBD

3.2.2 Single Load Infinite Bus (SLIB) playback studies

Single Load Infinite Bus (SLIB) playback validations were conducted to assess the transient behaviours of the CMLD and DERAEMO1 models.

For each of the disturbances listed in Table 7, representative network cases were created (accessing the pre-disturbance snapshot and isolating the buses of interest). An example is shown in Figure 9 for Cranbourne (CBTS), as applied in the 18/01/2018 disturbance. For each case, the recorded voltage and frequency at the relevant location was played back into a SLIB equivalent representation of the CMLD and DERAEMO1 models, and the active/reactive power responses of the models compared with observations.

Figure 9 Cranbourne network (CBTS) used for SLIB validation studies (18 January 2018)

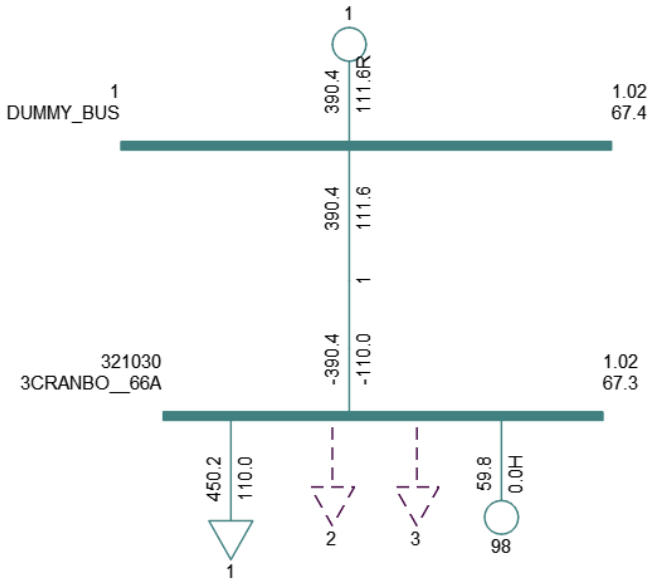

3.2.3 SLIB validation results

Figure 10 shows a typical example of the SLIB validation results. The measured voltage and frequency (which were played back into the CMLD and DERAEMO1 models) are shown in the top two panels. The middle two panels show the active and reactive power responses, comparing the measurements (black) with the CMLD+DPV model responses (blue) and the response of the original exponential (ZIP) load model (red), focusing on the first two seconds of transient response. The bottom two panels show the longer term response over the first sixty seconds post disturbance for both active and reactive power. General observations from all the SLIB studies include:

- **Reactive power:** The CMLD+DPV model provides a significant improvement in the representation of reactive power. The immediate transient response during and post-fault is much better represented (compared with the ZIP model). The CMLD+DPV model also provides a better representation of the steady state response (over the subsequent sixty seconds) compared with the ZIP model.
- **Active power:** The CMLD+DPV model provides a somewhat improved active power trajectory, better representing the rate of active power rise post fault, and steady state settling level of active power, compared with the ZIP model. Both models tend to underestimate the post fault clearance overshoot.

These observations were generally consistent across the SLIB cases studied; further detailed results are provided in Appendix A5.

Figure 10 18/01/2018 – Cranbourne (CBTS) – Typical example

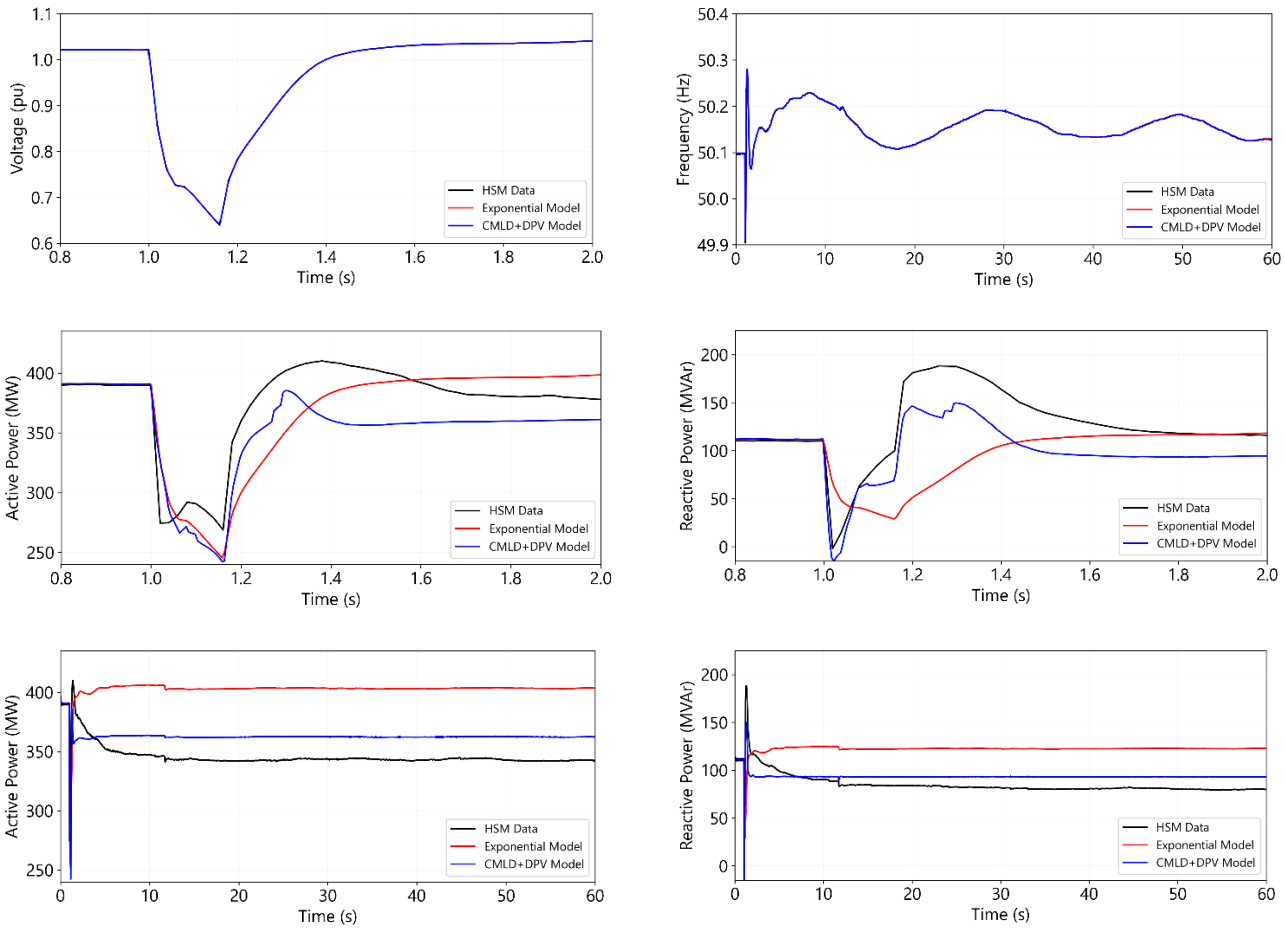

Table 9, Table 10, Table 11 and Table 12 provide a summary of the SLIB case findings. Results are categorised by whether they are better, as good, or worse than the previous exponential (ZIP) model, as well as by whether they provide a good, fair or poor match to the observed high speed monitoring (HSM) data, using the indicators as shown in the legend in Table 8. The transient behaviour was assessed based on the general shape of response during the contingency and the rate of recovery immediately (first 2 s) following the contingency compared to the HSM data. The steady state behaviour was assessed based on the settled value (10-60 s following the contingency) compared to the HSM data.

Table 8 Legend for tables below

✓	Better than Exponential model
-	At least as good as exponential model
✖	Worse than exponential model
	CMLD+DERAEMO1 is a good match to HSM
	CMLD+DERAEMO1 is a fair match to HSM
	CMLD+DERAEMO1 is a poor match to HSM

As shown in Table 9 and Table 10, the CMLD+DERAEMO1 model provides a better representation of active and reactive power in the transient timeframe than the ZIP model in all cases, and provides at least a fair representation of the HSM measurements in all cases. In some cases, the representation of the measured transient reactive power response is very good, and much improved compared with the ZIP model.

Table 9 Active power - Transient

Event date	Brooklyn (BLTS)	Cranbourne (CBTS)	Red Cliffs (RCTS)	Rowville (ROTS) / Springvale (SVTS)	Templestowe (TSTS)
25/07/2022 (night)	NA	NA	-	NA	NA
18/01/2018 (day)	✓	✓	NA	✓	-
31/01/2020 (day)	✓	✓	NA	✓	✓
8/03/2018 (night)	NA	NA	NA	✓	✓
18/02/2019 (night)	NA	NA	NA	✓	NA

Table 10 Reactive power - Transient

Event date	Brooklyn (BLTS)	Cranbourne (CBTS)	Red Cliffs (RCTS)	Rowville (ROTS) / Springvale (SVTS)	Templestowe (TSTS)
25/07/2022 (night)	NA	NA	✓	NA	NA
18/01/2018 (day)	✓	✓	NA	✓	✓
31/01/2020 (day)	✓	✓	NA	✓	✓
8/03/2018 (night)	NA	NA	NA	✓	✓
18/02/2019 (night)	NA	NA	NA	✓	NA

As shown in Table 11 and Table 12, in most cases the steady state active and reactive power is better represented by the CMLD+DERAEMO1 models compared with the ZIP model, and in some cases provides a very good match to the high speed monitoring data. In a few select cases, the CMLD+DERAEMO1 model is poorer than ZIP at representing the steady state observations.

Table 11 Active power – Steady State

Event date	Brooklyn (BLTS)	Cranbourne (CBTS)	Red Cliffs (RCTS)	Rowville (ROTS) / Springvale (SVTS)	Templestowe (TSTS)
25/07/2022 (night)	NA	NA	✓	NA	NA
18/01/2018 (day)	×	✓	NA	✓	✓
31/01/2020 (day)	✓	×	NA	×	-
8/03/2018 (night)	NA	NA	NA	✓	✓
18/02/2019 (night)	NA	NA	NA	-	NA

Table 12 Reactive power – Steady State

Event date	Brooklyn (BLTS)	Cranbourne (CBTS)	Red Cliffs (RCTS)	Rowville (ROTS) / Springvale (SVTS)	Templestowe (TSTS)
25/07/2022 (night)	NA	NA	×	NA	NA
18/01/2018 (day)	-	✓	NA	✓	✓
31/01/2020 (day)	-	×	NA	×	-
8/03/2018 (night)	NA	NA	NA	×	×
18/02/2019 (night)	NA	NA	NA	-	NA

SLIB testing findings

Based on these SLIB validation tests, the CMLD+DERAEMO1 models appear to generally provide a better representation of transient behaviours (compared with the previous ZIP model), especially for transient reactive power.

4 Active power recovery rates

Further testing of the models revealed that small differences in the rate of active power recovery between the CMLD and DERAEMO1 models can lead to important differences in system rate of change of frequency (RoCoF) and frequency outcomes. This has been influential when the models were applied to calculation of inertia requirements[22].

Following a deep voltage disturbance, the DERAEMO1 model active power recovers more slowly than the CMLD load model, as shown in Figure 11. The CMLD model is highly voltage dependent, and the active power response snaps back quickly to close to pre disturbance levels (with some accompanying dynamic behaviour) following a deep voltage sag. In contrast, the DERAEMO1 model active power recovery exhibits some delay, with active power showing a slower, ramped recovery post fault. This can create a short duration deficit in active power, which can exacerbate an under-frequency disturbance. This can be particularly important when power system inertia is low and the frequency response of the power system is more sensitive (which can be more likely in periods with large amounts of distributed PV operating, and therefore fewer synchronous units operating).

Review of the relevant parameters indicates that the recovery delays in the DERAEMO1 model appear suitable; they are representative of real measurement and processing delays and the ramp is consistent with similar inverter-based generation models.

[22] AEMO (December 2023) 2023 Inertia Report, Appendix A1, https://aemo.com.au/-/media/files/electricity/nem/security_and_reliability/system-strength-requirements/2023-inertia-report.pdf?la=en&hash=AF08771E3E52A9BF22D210F8C2CB203A . The assessment of frequency outcomes in this report considered the combined response of the CMLD and DER models, generator dynamic models and FFR settings of existing, committed, and anticipated batteries.

Figure 11 Example of active power recovery rates post fault

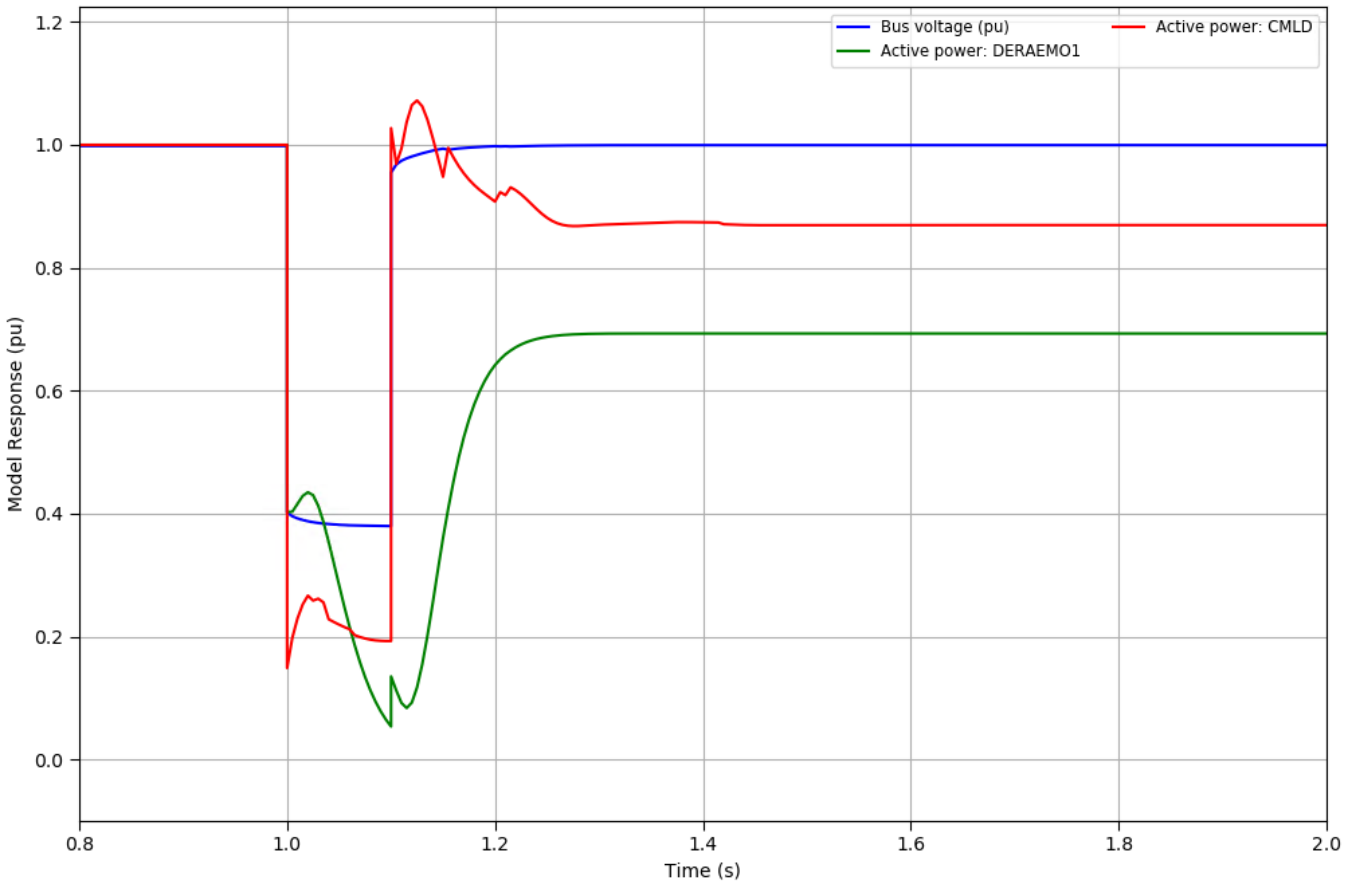

Figure 12 shows the current/output control block diagram as implemented in the DERAEMO1 model (sourced from the DER_A model developed by WECC[23]). There are a number of factors in the model which contribute to the delay in active power recovery, as listed in Table 13. The values in the DERAEMO1 model have been sourced from the NERC Reliability Guideline[24] and the inverter bench testing results.

Table 13 Factors in DERAEMO1 which influence active power recovery post fault

Parameter	Description	DERAEMO1 value	Source
Tv	Time constant on the output of the multiplier (tripping logic) block (s)	0.02	NERC Reliability Guideline
Rrpwr	Ramp rate for real power increase following a fault	10	Inverter bench test results
Trv	Voltage measurement transducer time constant (s)	0.02	NERC Reliability Guideline
Tp	Power measurement transducer time constant (s)	0.02	NERC Reliability Guideline
-	Voltage source at the output of the current control	-	-

[23] Proposal for DER_A model (19 June 2019) WECC REMTF, Pouyan Pourbeik, https://www.wecc.org/Reliability/DER_A_Final_061919.pdf

[24] Reliability Guideline – Parameterization of the DER_A Model (September 2019) NERC, https://www.nerc.com/comm/RSTC_Reliability_Guidelines/Reliability_Guideline_DER_A_Parameterization.pdf

Figure 12 DER model – Current/Output control

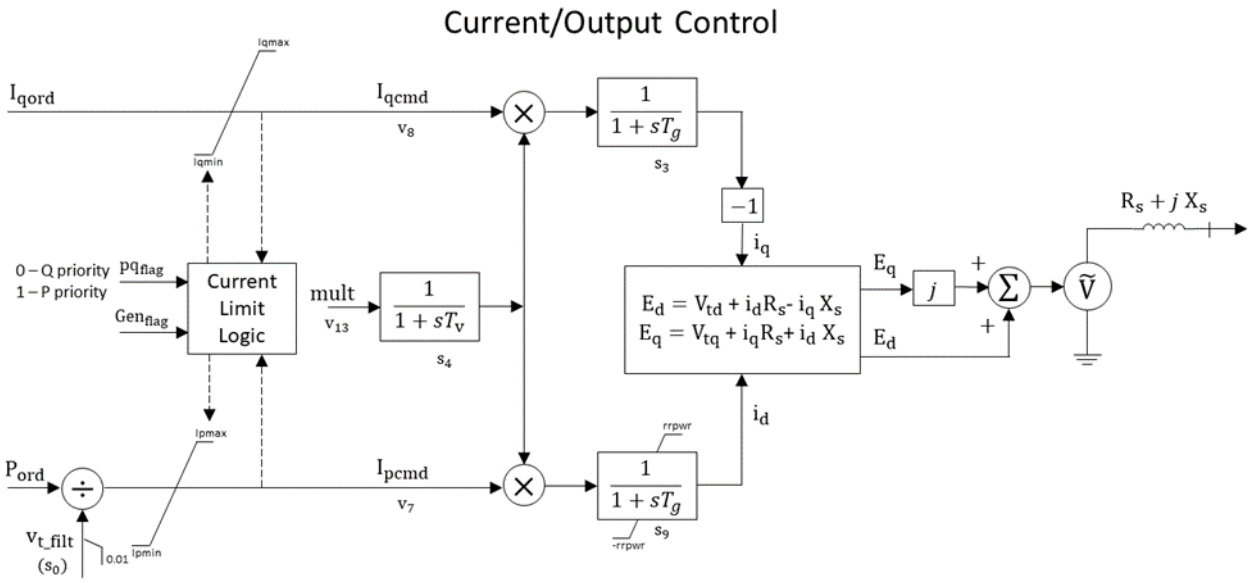

4.1.1 Bench testing of inverters

UNSW Sydney has conducted bench testing of numerous household distributed PV inverters[25]. These test observations have been used to inform parameters and behaviours for the DERAEMO1 model. The test results were interrogated to determine the speed of active power recovery post-disturbance.

Figure 13 shows an example test result for an inverter subjected to a 0.2pu voltage sag for 80ms. The inverter demonstrates an 80ms delay for the active power (Pg) to recover to the pre-disturbance level from when the voltage sag begins to be removed. In general, of the 46 inverters tested, most inverters showed a recovery delay in the range of 2 - 150ms, with an average recovery delay of 90ms. This is consistent with the recovery delay exhibited by the DERAEMO1 model (~100 ms).

[25] Addressing Barriers to Efficient Renewable Integration, at https://research.unsw.edu.au/projects/addressing-barriers-efficient-renewable-integration, and http://pvinverters.ee.unsw.edu.au/

Figure 13 Example inverter bench test result – 0.2pu sag for 80ms[26]

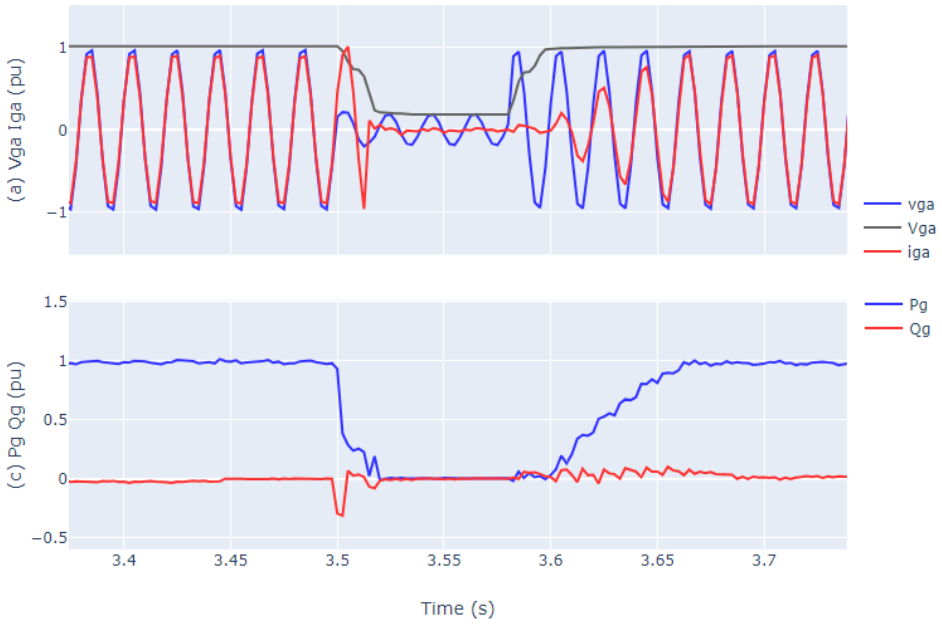

Active power rate of recovery

The rate of active power recovery of the DERAEMO1 model appears reasonable, given available evidence.

[26] Inverter 31, operating at full power.

5 Next Steps

This report summarises some recommended improvements to the parameters in the CMLD model. AEMO recommends that stakeholders adopt these updated parameters in any future studies if utilising these models.

The CMLD and DERAEMO1 models provide important improvements in load and DPV representation in power system studies compared with the earlier ZIP load models, but also have many remaining limitations, and should be applied with discretion and only when appropriate. Stakeholders retain responsibility for the validity of their studies, and should use appropriate discretion and due diligence when deciding whether to apply these models to their studies.

AEMO will continue to work with TNSPs on improvements to these models. Ongoing areas of work include:

- Integrating the DERAEMO1 and CMLD models into AMP (AEMO Modelling Platform) for streamlined and robust application of the models in future studies.
- Continue to support adoption of these models at AEMO and TNSPs, with continuous assessment and validation to ensure models are fit for purpose for the wide range of possible applications.
- Adjustments to the DERAEMO1 model to capture improving AS4777:2020 compliance[27].
- Additional bench testing of various loads (by University of Wollongong) to continue to inform load behaviour and further improvements to the CMLD model.
- Additional bench testing of DPV and distributed battery energy storage (BESS) inverters, to continue to inform DER behaviours and further improvements to the DERAEMO1 model.
- Testing to understand behaviour of EV chargers and inform development of suitable models to represent these in power system studies.

[27] AEMO (December 2023) Compliance of Distributed Energy Resources with Technical Settings: Update, https://aemo.com.au/-/media/files/initiatives/der/2023/oem_compliance_report_2023.pdf?la=en&hash=E6BEA93263DE58C64FCC957405808CA6

A1. DERAEMO1 summary

This Appendix provides a summary of the functionality of the DERAEMO1 model, intended to represent distributed PV in the NEM. The model is highly sensitive to voltage, and also has some frequency dependency. The most significant behaviours are outlined in the sections below. Appendix A2 outlines the parameter values used in this report.

A1.1 Under-voltage response

The under-voltage tripping behaviour is one of the most important aspects of the DPV model, and has been carefully tuned to match observations from inverter bench testing, and numerous field disturbances.

The voltage response of the model is primarily defined by the 'vrfrac' block, illustrated in Figure 14. This block represents both "momentary cessation" behaviour (where a proportion of inverters will temporarily reduce active power injection during a voltage excursion), and voltage tripping behaviour (a proportion of inverters will trip in response to a voltage excursion, and will not reconnect for the duration of the simulation). The vrfrac block operates as follows:

- The output of this block is a multiplier on the active power output of the model.
- As the bus voltage falls below vl1 (0.9pu), the active power output of the model reduces linearly (reaching zero at vl0 (~0.6pu)). This represents momentary cessation. If the bus voltage recovers within less than the time tvl1 (~0.03s), then the power output of the model will recover to pre-event levels.
- If the bus voltage remains below vl1 (0.9pu) for longer than the time tvl1 (~0.03s), the model will only partially recover, with active power following the red line when voltage recovers to pre-event levels. This represents tripping of a proportion of inverters. They will not reconnect for the duration of the simulation.
- If the bus voltage remains below vl0 (~0.6pu) for more than the time delay tvl0 (~2s), the entire DPV model will trip and remain at zero for the duration of the simulation, representing tripping of all inverters at the bus.

The proportion of inverters that do not trip is determined by the parameter 'vrfrac' (~0.7) (fraction of devices that recover following a fault), defined in Equation 1.

Figure 14 vrfrac block

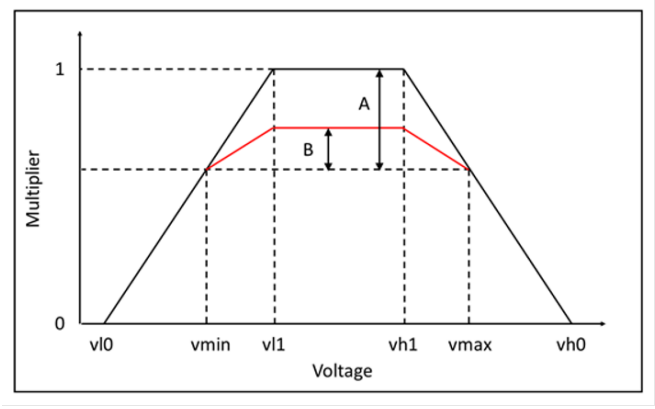

Equation 1:

$$B = Vrfrac\ x\ A = Vrfrac\left(\frac{vl1 - Vmin}{vl1 - vl0}\right) = Vrfrac\ (\frac{vh1 - Vmax}{vh1 - vh0})$$

Inverters installed prior to October 2016 were installed under the 2005 Australian Standard (AS4777.3:2005). Inverters installed after that date were installed under the 2015 standard (AS/NZS4777.2:2015). Each inverter type has different behaviours based on the requirements of those standards, and based on observed behaviour from inverters of that vintage during field disturbances. The model parameters are a weighted average of the two, depending on the proportion of each inverter type installed at the date of the relevant study. Table 14 lists the parameters estimated for inverters under each standard, and provides the weighted average estimated for the present day mix in the NEM.

Table 14 vrfrac block parameters – under-voltage behaviour

Parameter	Description	2005 standard	2015 standard	Present Day Mix	Comments
vl1	1st LV Setpoint	0.9 pu	0.9 pu	0.9 pu	Based on inverter bench testing. Inverters of both types begin to disconnect at 0.9pu.
vl0	2nd LV Setpoint	0.75 pu	0.5 pu	0.5 to 0.7 pu	Estimates from Australian Standards provided a starting point: AS4777.3-2005 requires that if voltage falls below 200V (0.86pu), inverter disconnects within 2s. AS/NZS 4777.2:2015 requires that if voltage falls below 180V (0.78pu) for more than 1s, then inverter disconnects in a maximum of 2s. vl0 was then tuned, keeping vl1 at 0.9pu, to adjust the vl1-vl0 gradient to match overall PV tripping observed in field disturbances.
tvl1	1st LV trip delay	0.027 s	0.037 s	0.03 to 0.04 s	Based on inverter bench testing (average disconnection time for under-voltage step 230V to 50V for 100ms)
tvl0	2nd LV trip delay	1.58 s	1.77 s	1.68 to 1.74 s	Based on inverter bench testing (average disconnection time for under-voltage ramp 230V to 160V for 10s, measuring delay from when voltage falls below thresholds defined in standards)
vrfrac	Fraction of devices that recover following a voltage event	0.625	0.713	0.67 to 0.70	Based on inverter bench testing (120ms voltage sags to varying levels between 0.9pu and 0.2pu) to determine fraction that recover, and fine-tuned against field disturbances in conjunction with vl0.

A1.2 Over-voltage response

The over-voltage response of the DPV model mirrors the under-voltage behaviour of the vrfrac block. For over-voltage excursions, the behaviour of the DPV model can be described as follows:

- As the bus voltage rises above vh1 (1.13pu), the active power output of the model reduces linearly (reaching zero at vh0, 1.18pu). This represents momentary cessation. If the bus voltage recovers below vh1 within less than the time delay tvh1 (~2s), then the power output of the model will recover to pre-event levels.
- If the bus voltage remains above vh1 (1.13pu) for longer than the time delay tvh1 (~2s), the model will only partially recover, with active power following the red line when voltage recovers to pre-event levels. This represents tripping of a proportion of inverters. They will not reconnect for the duration of the simulation.
- If the bus voltage remains above vh0 (~1.18pu) for more than the time delay tvh0 (~0.4s), the entire DPV model will trip and remain at zero for the duration of the simulation, representing tripping of all inverters at the bus.

The parameters for over-voltage behaviour are summarised in Table 15. The vrfrac parameter (fraction of devices that do not trip and recover) is identical for under-voltage and over-voltage (~0.7).

Table 15 vrfrac block parameters – over-voltage behaviour

Parameter	Description	2005 standard	2015 standard	Present Day Mix	Comments
vh1	1st HV Setpoint	1.13 pu	1.13 pu	1.13 pu	AS/NZS 4777.2:2015 requires that if voltage exceeds 260V (1.13pu) for more than 1s, then disconnect inverters in a maximum of 2s. AS4777.3-2005 requires that if voltage exceeds 270V (1.17pu), disconnect inverters within 2s. The value from the 2015 standard was applied, since this represents the earliest over-voltage where a model response should begin.
vh0	2nd HV Setpoint	1.18 pu	1.18 pu	1.18 pu	AS/NZS 4777.2:2015 requires that if voltage exceeds 265V (1.15pu) disconnect inverters within 0.2s. This provided a starting point. Vh0 was fine tuned in validation studies, to decrease the vh1-vh0 gradient to make the over-voltage trip settings less sensitive (representing a proportion of inverters under the 2005 standard that may not feature this fast trip setting).
tvh1	1st HV trip delay	1.94 s	1.87 s	1.89 to 1.91 s	Based on inverter bench testing (average disconnection time for over-voltage step 230V to 260V)
tvh0	2nd HV trip delay	0.88 s	0.16 s	0.3 to 0.5 s	Based on inverter bench testing (average disconnection time for over-voltage step 230V to 270V)

Due to limited field observations, the over-voltage behaviour of the model is based heavily on specifications in the Australian Standards (the model represents the behaviour required in the 2015 standard, with the thresholds and timers made somewhat higher and longer to represent the somewhat more relaxed trip settings in the 2005 standard). The under-voltage behaviour of the model is based more strongly on field observations and bench testing observations.

A1.3 Reactive Power-Voltage response

The DERAEMO1 model has the potential to represent Volt-Var responses. This power quality mode has been required for new connections by most distribution network service providers in recent years, and is mandatory in the latest AS/NZS4777.2:2020. However, this response is not enabled in the DERAEMO1 model in this version. This is for the following reasons:

1. Inverter bench testing has shown that the Volt-Var response of inverters, once activated, takes seconds to respond. There is little evidence to indicate inverters will provide voltage support during a fault (which may only last ~100ms).
2. Reactive power injection/consumption in the distribution network is unlikely to result in changes to voltages/reactive power in the transmission network. The DERAEMO1 model is connected at higher voltage buses, to represent the aggregate behaviour of distributed PV connected downstream, as observed in the transmission network.
3. Field measurements indicate low compliance in delivery of Volt-Var response (70-80% of inverters are not delivering this response)[28]

This can be reconsidered in future model versions, particularly if inverter compliance in delivery of this power quality mode improves, and further evidence becomes available on how Volt-Var response impacts disturbance behaviour improves. The reduction in active power injection when inverters are preferencing delivery of reactive power under this power quality mode could be an important feature, to accurately represent behaviour visible in the transmission network.

A1.4 Under-frequency response

The DERAEMO1 model includes thirteen under-frequency trip stages. A proportion of the model will trip as frequency falls below 49Hz (with varying time delays as frequency falls further) and will not recover for the duration of the simulation. The most influential under-frequency tripping stages (above 48Hz) are listed in Table 16. These are based on the proportion of older inverters (installed under the 2005 standard) which are known to have trip settings at these levels based on manufacturer surveys. The same trip settings are also applied to the fleet of newer inverters (installed under the 2015 standard) but with trip percentages halved. This has been tuned to match field observations, and represents the somewhat improved frequency behaviour of newer inverters, but with poor compliance with the 2015 standard. See Appendix A2.4 for the complete set of under-frequency tripping parameters.

Table 16 Under-frequency tripping stages

			Percentage that disconnects (fracl_fl)		
Trip Stage	**Frequency Trip Setting (Hz) (fl)**	**Trip Delay (s) (tfl)**	**2005 standard***	**2015 standard***	**Present day mix**
Trip 1	49.6	1.9	2%	1%	1 to 1.5%
Trip 2	49.01	0.18	0.7 to 4%	0.4 to 2%	0.5 to 3%

[28] AEMO (April 2023) Compliance of Distributed Energy Resources with Technical Settings, https://aemo.com.au/-/media/files/initiatives/der/2023/compliance-of-der-with-technical-settings.pdf?la=en&hash=FC30DF5A3B9EF853093709012242D897

			Percentage that disconnects (fracl_fl)		
Trip 3	49	0.06	9 to 16%	5 to 8%	6 to 12%
Trip 4	49	1.96	2.5 to 8%	1.3 to 4%	2 to 5%
Trip 5	49	2	0 to 0.3%	0 to 0.2%	0 to 0.2%
Trip 6	48.52	2	0.5 to 1.3%	0.3 to 0.7%	0 to 1%

* Varies region to region depending on proportion of relevant manufacturer products installed under the 2005 standard in each region

The DERAEMO1 model does not have any other response to under-frequency.

A1.5 Over-frequency response

The DERAEMO1 model includes thirteen over-frequency trip stages. The most influential under-frequency tripping stages (those below 52Hz) are listed in Table 17. These were determined similarly to under-frequency trip settings. See Appendix A2.4 for the complete set of over-frequency tripping parameters.

Table 17 Over-frequency tripping stages

			Percentage that disconnects (frac_fh)		
Trip Stage	**Frequency Trip Setting (Hz) (fh)**	**Trip Delay (s) (tfh)**	**2005 standard**	**2015 standard**	**Present day mix**
Trip 1	50.5	1.9	7%	3.5%	4 to 5%
Trip 2	50.8	1.9	5%	1%	2 to 3%
Trip 3	51	0.06	3 to 9%	4 to 7%	4 to 8%
Trip 4	51	1.96	0.7 to 6%	1 to 4%	1 to 5%
Trip 5	51	2	0 to 0.2%	0 to 0.2%	0 to 0.2%
Trip 6	51.6	2	0.5 to 1.3%	0.3 to 0.7%	0 to 1%
Trip 7	51.9	1.8	1 to 8%	0.5 to 4%	1 to 5%

The DERAEMO1 model also includes an over-frequency droop response, as required in the 2015 standard. As frequency exceeds 50.25Hz, the model active power will reduce linearly (reaching zero at 52 Hz). The active power will not recover from the lowest level reached for the duration of the simulation, representing the 60s delay required in the standard. The amount of response is scaled by the proportion of inverters in the simulation installed under the 2015 standard (since this response was not required from older inverters), and is also scaled down representing poor compliance with the 2015 standard (calibrated based on observations in a number of field disturbances).

For severe over-frequency disturbances, the over-frequency tripping and over-frequency droop curtailment response have been observed to be approximately similar in magnitude, contributing relatively equally to the reduction in active power from the model.

A1.6 Response to Rate of Change of Frequency (RoCoF)

The DERAEMO model also represents a proportion of inverters tripping if certain RoCoF thresholds are exceeded, as listed in Table 18. These are based on observations from inverter bench testing. These trip settings apply to both increasing and decreasing RoCoF.

Table 18 RoCoF trip stages

			Percentage that disconnects (frac_RoCoF)		
Trip Stage	**RoCoF Trip Setting (RoCoF)**	**Trip Delay (s) (tRoCoF)**	**2005 standard**	**2015 standard**	**Present day mix**
Trip 1	0.4 Hz/s (0.008 pu/s)	1.41 s	3.5 to 4%	3.5 to 4%	3.5 to 4%
Trip 2	1 Hz/s (0.02 pu/s)	0.83 s	4 to 10%	4 to 10%	4 to 10%

A2. DERAEMO1 parameters

The section summarises the DERAEMO1 parameters used in VNI export transient stability limit (see Table 5) studies outlined in this report. As the DERAEMO1 parameters evolve over time, updates to these parameters will be released through the AEMO Modelling Platform (AMP).

A2.1 Voltage control parameters

Some of the voltage control parameters that are redundant in the DERAEMO1 model implementation have changed in this release and have now been set to zero. These changes have no impact on model behaviour, so the response of the DERAEMO1 model will be identical to the previous version of the DERAEMO1 model.

Table 19 Voltage Control Parameters in the DERAEMO1 model (identical for all regions)

Parameter	Name	Description	Value
M	PfFlag	reactive power control mode: • 1 : constant power factor mode • 0 : constant Q control mode	1
J	Trv	(s) voltage measurement transducer time constant	0.02
J+2	dbd1	(pu) lower voltage deadband (<= 0)	0
J+3	dbd2	(pu) upper voltage deadband (> 0)	0
J+5	Vref	(pu) user specified voltage set-point	1
J+7	Tiq	(s) Q-control time constant	0.02
J+31	Kqv1	(pu) proportional voltage control gain for reactive power reduction	0
J+32	Kqv2	(pu) proportional voltage control gain for reactive power increase	0
J+39	Iqh1	(pu) upper limit on reactive current injection Iqinj	0
J+40	Iql1	(pu) lower limit on reactive current injection Iqinj	0

A2.2 Voltage tripping parameters

Table 20 Voltage tripping parameters in the DERAEMO1 model (identical for all regions)

Parameter	Name	Description	Value
M+4	VtripFlag	flag to enable/disable voltage trip logic: • 1 : enable • 0 : disable	1
J+23	vl1	(pu) second breakpoint for low voltage cut-out (vl1 >vl0)	0.90

Table 21 Voltage tripping parameters in the DERAEMO1 model that vary between regions

Parameter	Name	Description	Value				
			NSW	VIC	QLD	SA	TAS
J+22	vl0	(pu) first breakpoint for low voltage cut-out	0.548	0.556	0.568	0.570	0.589

Parameter	Name	Description	Value				
			NSW	VIC	QLD	SA	TAS
J+24	vh0	(pu) first breakpoint for high voltage cut-out	1.180	1.180	1.180	1.180	1.180
J+25	vh1	(pu) second breakpoint for high voltage cut-out (vh1< vh0)	1.130	1.130	1.131	1.130	1.130
J+26	tvl0	(s) low voltage cut-out timer corresponding to voltage vl0	1.731	1.725	1.716	1.714	1.700
J+27	tvl1	(s) low voltage cut-out timer corresponding to voltage vl1	0.035	0.035	0.035	0.034	0.034
J+28	tvh0	(s) high voltage cut-out timer corresponding to voltage vh0	0.297	0.321	0.356	0.361	0.416
J+29	tvh1	(s) high voltage cut-out timer corresponding to voltage vh1	1.887	1.889	1.893	1.893	1.899
J+30	vrfrac	fraction of devices that recovers after voltage comes back within vl1 < V < vh1 (0 <= Vrfrac <= 1)	0.696	0.693	0.692	0.688	0.682

A2.3 Frequency control parameters

Table 22 Frequency control parameters in the DERAEMO1 model (identical for all regions)

Parameter	Name	Description	Value
M+1	FreqFlag	flag to enable/disable frequency droop control: • 1 : frequency control enabled • 0 : frequency control disabled	1
J+1	Trf	(s) frequency measurement transducer time constant	0.02
J+4	Trocof	(s) RoCoF Filter time constant	0.02
J+9	Dup	(pu) reciprocal of droop for under-frequency conditions (> 0)	0
J+10	fdbd1	(pu) deadband for frequency control, lower threshold (<= 0)	-0.005
J+11	fdbd2	(pu) deadband for frequency control, upper threshold (>= 0)	1
J+12	femax	(pu) freq. error upper limit	99
J+13	femin	(pu) freq. error lower limit	-99
J+14	Pmax	(pu) max. power limit	1
J+15	Pmin	(pu) min. power limit	0
J+16	dPmax	(pu/s) power reference maximum ramp rate (> 0)	0
J+17	dPmin	(pu/s) Power reference minimum ramp rate (< 0)	-99
J+18	Tpord	(s) Power filter time constant	0.02
J+19	Kpg	(pu) PI controller proportional gain	0
J+20	Kig	(pu) PI controller integral gain	10

Table 23 Frequency control parameters in the DERAEMO1 model that vary between regions

Parameter	Name	Description	Value				
			NSW	VIC	QLD	SA	TAS
J+8	Ddn	(pu) reciprocal of droop for over-frequency conditions (< 0)	8.09	7.75	7.49	7.19	6.43

A2.4 Frequency tripping parameters

Table 24 Frequency tripping parameters in the DERAEMO1 model (identical for all regions)

Parameter	Name	Description	Value
M+5	FtripFlag	flag to enable/disable frequency trip logic: • 1 : enable • 0 : disable	1
J+38	Vpr	(pu) voltage below which frequency tripping is disabled	0.90
J+41	fl1	(Hz) low frequency trip limit 1	49.60
J+42	fl2	(Hz) low frequency trip limit 2	49.01
J+43	fl3	(Hz) low frequency trip limit 3	49.00
J+44	fl4	(Hz) low frequency trip limit 4	49.00
J+45	fl5	(Hz) low frequency trip limit 5	49.00
J+46	fl6	(Hz) low frequency trip limit 6	48.52
J+47	fl7	(Hz) low frequency trip limit 7	47.60
J+48	fl8	(Hz) low frequency trip limit 8	47.55
J+49	fl9	(Hz) low frequency trip limit 9	47.50
J+50	fl10	(Hz) low frequency trip limit 10	47.10
J+51	fl11	(Hz) low frequency trip limit 11	47.00
J+52	fl12	(Hz) low frequency trip limit 12	47.00
J+53	fl13	(Hz) low frequency trip limit 13	47.00
J+54	tfl1	(s) pick-up time for low frequency trip 1	1.90
J+55	tfl2	(s) pick-up time for low frequency trip 2	0.18
J+56	tfl3	(s) pick-up time for low frequency trip 3	0.06
J+57	tfl4	(s) pick-up time for low frequency trip 4	1.96
J+58	tfl5	(s) pick-up time for low frequency trip 5	2.00
J+59	tfl6	(s) pick-up time for low frequency trip 6	2.00
J+60	tfl7	(s) pick-up time for low frequency trip 7	1.80
J+61	tfl8	(s) pick-up time for low frequency trip 8	0.20
J+62	tfl9	(s) pick-up time for low frequency trip 9	1.80
J+63	tfl10	(s) pick-up time for low frequency trip 10	1.80
J+64	tfl11	(s) pick-up time for low frequency trip 11	1.60
J+65	tfl12	(s) pick-up time for low frequency trip 12	0.10
J+66	tfl13	(s) pick-up time for low frequency trip 13	1.65
J+80	fh1	(Hz) high frequency trip limit 1	50.50
J+81	fh2	(Hz) high frequency trip limit 2	50.80
J+82	fh3	(Hz) high frequency trip limit 3	51
J+83	fh4	(Hz) high frequency trip limit 4	51
J+84	fh5	(Hz) high frequency trip limit 5	51
J+85	fh6	(Hz) high frequency trip limit 6	51.58
J+86	fh7	(Hz) high frequency trip limit 7	51.90

Parameter	Name	Description	Value
J+87	fh8	(Hz) high frequency trip limit 8	52.00
J+88	fh9	(Hz) high frequency trip limit 9	52.00
J+89	fh10	(Hz) high frequency trip limit 10	52.45
J+90	fh11	(Hz) high frequency trip limit 11	52.90
J+91	fh12	(Hz) high frequency trip limit 12	53
J+92	fh13	(Hz) high frequency trip limit 13	53
J+93	tfh1	(s) pick-up time for high frequency trip 1	1.9
J+94	tfh2	(s) pick-up time for high frequency trip 2	1.9
J+95	tfh3	(s) pick-up time for high frequency trip 3	0.06
J+96	tfh4	(s) pick-up time for high frequency trip 4	1.96
J+97	tfh5	(s) pick-up time for high frequency trip 5	2
J+98	tfh6	(s) pick-up time for high frequency trip 6	2
J+99	tfh7	(s) pick-up time for high frequency trip 7	1.8
J+100	tfh8	(s) pick-up time for high frequency trip 8	1.6
J+101	tfh9	(s) pick-up time for high frequency trip 9	0.15
J+102	tfh10	(s) pick-up time for high frequency trip 10	0.2
J+103	tfh11	(s) pick-up time for high frequency trip 11	1.8
J+104	tfh12	(s) pick-up time for high frequency trip 12	0.1
J+105	tfh13	(s) pick-up time for high frequency trip 13	0.16

Table 25 Frequency tripping parameters in the DERAEMO1 model that vary between regions

Parameter	Name	Description	Value				
			NSW	VIC	QLD	SA	TAS
J+67	frac_fl1	fraction for low frequency trip 1	1.19%	1.23%	1.26%	1.28%	1.36%
J+68	frac_fl2	fraction for low frequency trip 2	1.17%	2.54%	1.35%	0.94%	0.51%
J+69	frac_fl3	fraction for low frequency trip 3	7.68%	8.21%	5.86%	6.19%	11.18%
J+70	frac_fl4	fraction for low frequency trip 4	2.34%	5.08%	2.17%	1.64%	2.41%
J+71	frac_fl5	fraction for low frequency trip 5	0.06%	0.18%	0.06%	0.18%	0.00%
J+72	frac_fl6	fraction for low frequency trip 6	0.77%	0.31%	0.50%	0.58%	0.48%
J+73	frac_fl7	fraction for low frequency trip 7	4.88%	2.08%	1.20%	2.05%	0.68%
J+74	frac_fl8	fraction for low frequency trip 8	1.73%	1.35%	1.51%	2.63%	1.36%
J+75	frac_fl9	fraction for low frequency trip 9	4.82%	3.19%	6.62%	2.82%	5.16%
J+76	frac_fl10	fraction for low frequency trip 10	5.48%	5.64%	11.86%	4.93%	14.86%
J+77	frac_fl11	fraction for low frequency trip 11	0.83%	1.10%	0.50%	0.51%	0.07%
J+78	frac_fl12	fraction for low frequency trip 12	29.00%	30.76%	30.52%	40.67%	30.13%
J+79	frac_fl13	fraction for low frequency trip 13	40.04%	38.34%	36.58%	35.59%	31.82%
J+106	frac_fh1	fraction for high frequency trip 1	4.17%	4.29%	4.41%	4.48%	4.75%
J+107	frac_fh2	fraction for high frequency trip 2	1.76%	1.90%	2.08%	2.12%	2.43%
J+108	frac_fh3	fraction for high frequency trip 3	6.04%	7.56%	3.95%	3.77%	7.73%

Parameter	Name	Description	Value				
			NSW	VIC	QLD	SA	TAS
J+109	frac_fh4	fraction for high frequency trip 4	1.84%	4.68%	1.46%	1.00%	1.67%
J+110	frac_fh5	fraction for high frequency trip 5	0.04%	0.16%	0.04%	0.11%	0.00%
J+111	frac_fh6	fraction for high frequency trip 6	0.77%	0.31%	0.50%	0.58%	0.48%
J+112	frac_fh7	fraction for high frequency trip 7	4.88%	2.08%	1.20%	2.05%	0.68%
J+113	frac_fh8	fraction for high frequency trip 8	5.66%	4.29%	8.14%	5.44%	5.23%
J+114	frac_fh9	fraction for high frequency trip 9	0.00%	0.00%	1.24%	0.00%	0.00%
J+115	frac_fh10	fraction for high frequency trip 10	1.73%	1.35%	11.86%	4.93%	1.36%
J+116	frac_fh11	fraction for high frequency trip 11	5.48%	5.64%	0.50%	0.51%	14.86%
J+117	frac_fh12	fraction for high frequency trip 12	29.00%	30.76%	30.52%	40.67%	30.13%
J+118	frac_fh13	fraction for high frequency trip 13	38.63%	36.98%	34.09%	34.34%	30.69%

A2.5 RoCoF tripping parameters

Table 26 Frequency tripping parameters in the DERAEMO1 model (identical for all regions)

Parameter	Name	Description	Value
J+119	RoCoF_1	(pu/s)[29] RoCoF trip limit 1	0.008
J+120	RoCoF_2	(pu/s) RoCoF trip limit 2	0.02
J+121	RoCoF_3	(pu/s) RoCoF trip limit 3	0.08
J+122	tRoCoF_1	(s) pick up time for RoCoF trip 1	1.41
J+123	tRoCoF_2	(s) pick up time for RoCoF trip 2	0.83
J+124	tRoCoF_3	(s) pick up time for RoCoF trip 3	0.29

Table 27 Frequency tripping parameters in the DERAEMO1 model that vary between regions

Parameter	Name	Description	Value				
			NSW	VIC	QLD	SA	TAS
J+125	frac_RoCOF_1	fraction for RoCoF trip 1	3.72%	3.60%	4.03%	3.53%	3.56%
J+126	frac_RoCOF_2	fraction for RoCoF trip 2	4.37%	4.62%	9.71%	4.49%	7.32%
J+127	frac_RoCOF_3	fraction for RoCoF trip 3	0.00%	0.00%	0.00%	0.00%	0.00%

[29] Base frequency is 50 Hz

A3. CMLD summary

This Appendix provides a summary of the functionality of the CMLD model, intended to represent composite load in the NEM.

A3.1 CMLD overview

The composite load model (CMLD) breaks load down into six components: Motor A, Motor B, Motor C, Motor D, power electronics, and static load. Each model component is represented as follows:

- The Motor A, B and C components are represented in the model with motor models with varying inertia, impedance, and torque properties.
- Motor D is a specially developed performance model, based on laboratory tests, designed to represent single phase residential and light commercial refrigerator compressor motors which are prone to stalling behaviour (this component is believed to be small in Australia).
- The power electronics component includes under-voltage tripping behaviour, but is otherwise relatively insensitive to voltage or frequency.
- The static load is represented by a ZIP model, which does not have any tripping parameters, but scales active power with bus voltage.

The CMLD model parameters are intended to represent aggregate load behaviour.

A3.2 Under-voltage response of CMLD

The most important feature of the CMLD model is the under-voltage trip settings. These are crucial to represent aggregate load loss in severe under-voltage events, and accurately represent the net continency that can occur when distributed PV and load interact during a fault. This is a key distinguishing factor between CMLD and the previously used ZIP model (which cannot represent load tripping in severe voltage disturbances). The under-voltage trip settings are the main reason why it is important to use the CMLD model when applying the DERAEMO1 model to represent distributed PV, and a significant reason why the CMLD model provides an important improvement over the previous ZIP model.

The under-voltage trip settings applied to each component of the model are listed in Table 1. A percentage of the model (Ftr) will disconnect if the bus voltage remains below the trip voltage (Vtr) for longer than the trip delay time (Ttr). Some components will reconnect as indicated in the fifth column. These components will reconnect if voltages recover above required thresholds (0.6 to 0.75 pu, not shown) within the required time (0.05s to 0.11s, not shown), which does occur for typical transmission faults.

Table 1 - CMLD under-voltage trip stages

	Trip Voltage (pu) (Vtr)	Trip Delay (s) (Ttr)	Percentage that disconnects (Ftr)	Does it Reconnect?	Load proportion (%) (annual average)
Motor A 1st Setpoint	0.75	0.06	10%	No	12.5 to 15.3%
Motor A 2nd Setpoint	0.62	0.021	20%	Yes	
Motor B 1st Setpoint	0.7	0.02	10%	Yes	15.5 to 23.7%
Motor B 2nd Setpoint	0.45	0.021	20%	Yes	
Motor C 1st Setpoint	0.8	0.03	10%	No	12.4 to 13.9%
Motor C 2nd Setpoint	0.5	0.03	20%	Yes	
Motor D 1st Setpoint	0.6	0.02	33%	No	0.2 to 0.4%
Power Electronic Load	0.85 to 0.5	-	(30%)	No	33.7 to 15.3%
Static load	None	None	None	None	14.1 to 21.4%

For Power Electronic load, the proportion that trips reduces linearly from 100% to 0% as voltage reduces from 0.85pu to 0.5pu. The fraction that then reconnects following a fault is 70%. This means that 30% of the power electronics load remains disconnected.

The tripping components of the load model represent aggregate tripping behaviour, calibrated to match aggregate field observations in numerous field disturbances. They do not represent actual trip settings on individual devices.

A3.2.1 General voltage response (beyond tripping)

The static load model component does not include any trip settings, but is sensitive to bus voltage (scaling to increase active power when voltage is high, and decreasing active power when voltage is low). The Motor A, B and C components of the model are also somewhat sensitive to bus voltages. If the fraction of load in the static load component is large, this voltage response can dominate the response of the CMLD model, even during severe frequency disturbances.

A3.3 Over-voltage response of CMLD

There are no over-voltage tripping parameters in the CMLD model. As for under-voltage, the active power response from the static load model scales with voltage, and this can dominate the response of the load model.

A3.4 Frequency response of CMLD

The Motor B, C and D and components of CMLD deliver a small amount of load relief (increase in active power as frequency rises and decrease in active power as frequency falls). The Motor B, C and D components of the model reduce their load by 1-2% for every 0.5 Hz decline in frequency. These Motor components typically contribute 30-

50% of the power system load, so this equates to approximately the 0.5% load relief factor[30] assumed by AEMO for the NEM[31].

The same is delivered in reverse during over-frequency events.

The power electronic and static load components do not respond to frequency at all. The Motor A component demonstrates a very small change in active power when exposed to a changing frequency.

The CMLD model does not have explicit frequency or RoCoF tripping parameters.

In general, the voltage response of the load model is more influential than the frequency response of the load model.

[30] For a 1% change in frequency (0.5Hz), the total demand is assumed to change by 0.5%.

[31] AEMO, Load Relief, https://aemo.com.au/en/energy-systems/electricity/national-electricity-market-nem/system-operations/ancillary-services/load-relief

A4. CMLD Parameters (version 2)

This section summarises the recommended version 2 input parameters for the CMLD model for application in the NEM.

A4.1 CMLD composition parameters

A4.1.1 Large Industrial Load (LIL) composition parameters

Where there is a known Large Industrial Load (LIL) at a single transmission bus that does not already have a bespoke load model, the composition parameters summarised in Table 28 are applied.

Table 28 Load composition parameters for Auxiliary and Large Industrial Loads

	Auxiliary loads	Non-metal manufacturing	Metal manufacturing	Water pumping	Metal ore mining	Paper milling	Metal smelting	LNG
Motor A	5%	15%	20%	0%	15%	10%	10%	20%
Motor B	50%	25%	25%	0%	30%	25%	0%	25%
Motor C	25%	40%	25%	90%	30%	40%	0%	45%
Motor D	0%	0%	0%	0%	0%	0%	0%	0%
Power Electronic	15%	15%	25%	10%	20%	20%	15%	10%
Constant Current	5%	5%	5%	0%	5%	5%	75%	0%
Constant Impedance	0%	0%	0%	0%	0%	0%	0%	0%

A4.1.2 General end-use load composition parameters

All other loads are considered “general” load, and assigned the region specific composition parameters summarised in Table 29 and Table 30.

Table 29 Load composition parameters for general end-use-load – Annual average

	NSW	VIC	QLD	SA
Motor A	15.2%	15.3%	13.3%	12.5%
Motor B	16.6%	18.7%	23.7%	16.5%
Motor C	12.9%	12.4%	13.9%	12.8%
Motor D	0.2%	0.2%	0.2%	0.4%
Power Electronic	33.7%	35.0%	34.7%	40.1%
Constant Current	4.5%	4.6%	4.1%	3.8%
Constant Impedance	16.9%	13.9%	10.0%	13.9%

Table 30 Load composition parameters for general end-use-load – Peak Summer

	NSW	VIC	QLD	SA
Motor A	16.1%	15.2%	13.1%	11.3%
Motor B	16.4%	19.6%	24.5%	17.2%
Motor C	12.3%	11.2%	12.5%	11.7%
Motor D	3.0%	2.9%	2.4%	3.2%
Power Electronic	34.0%	35.2%	35.9%	42.0%
Constant Current	3.8%	3.8%	3.5%	3.1%
Constant Impedance	14.4%	12.1%	8.1%	11.5%

A4.2 CMLD feeder parameters

The CMLD model includes an equivalent representation of the feeder. The recommended parameters are summarised in the tables below.

Table 31 Feeder configuration parameters (depending on load type)

CON	Parameter	Description	Units	General load	Auxiliary load	Large Industrial Loads
J+2	Rfdr	Feeder resistance	pu on load base	0.04	0	0.01
J+3	Xfdr	Feeder reactance	pu on load base	0.04	0	0.01
J+5	Xxf	Transformer reactance	pu on load base*	0.08	0.06	0.08
J+8	LTC	LTC flag	1 = active 0 = inactive	0	0	0

* A feeder with a transformer reactance of zero bypasses the step-down transformer within the CMLD model.

Table 32 Common feeder parameters

CON	Parameters	Description	Value
J	LoadBase	Load base for xfr & feeder - MVA or calculated if <= 0	-0.8
J+1	compB	Substation compensation B - pu on load base	0
J+4	Fb	Not used - Fb = 0.0	0.75
J+6	Tfixhs	High side fixed transformer tap	1
J+7	Tfixls	Low side fixed transformer tap	1
J+9	Tmin	LTC min tap (on low side)	0.9
J+10	Tmax	LTC max tap (on low side)	1.1
J+11	Step	LTC Tstep (on low side)	0.00625
J+12	Vmin	Min value of V target range on xfr low side	1
J+13	Vmax	Max value of V target range on xfr low side	1.02
J+14	TD	LTC control time delay - s	30
J+15	TC	LTC tap adjustment time delay - s	5
J+16	Rcmp	xfr compensating R - pu on load base	0
J+17	Xcmp	xfr compensating X - pu on load base	0

A4.3 CMLD performance parameters

The tables below provide the recommended version 2 parameters to represent the performance of each of the CMLD model components.

Table 33 Power electronics performance parameters

CON	Parameters	Description	Value
J+23	PFel	Electronic load power factor	1
J+24	Vd1	Voltage electronic loads start to drop	0.85
J+25	Vd2	Voltage all electronic load has dropped	0.5
J+132	frcel	Fraction electronic load that can reconnect	0.7

Table 34 Static load performance parameters

CON	Parameters	Description	Value
J+26	PFs	Static load lower factor	1
J+27	P1e	First exponent for static load P	1
J+29	P2e	Second exponent for static load P	2
J+31	Pfrq	Frequency sensitivity for static P	0
J+32	Q1e	First exponent for static load Q	1
J+34	Q2e	Second exponent for static load Q	2
J+36	Qfrq	Frequency sensitivity for static load Q	-1

Table 35 Motor A performance parameters

CON	Parameters	Description	Value
J+37	Mtyp	Motor A phase - always 3	3
J+38	LF	Motor A real power to power base ratio	0.75
J+39	Ra	Motor A stator resistance - pu on motor base	0.02
J+40	X	Motor A synchronous reactance - pu	1.8
J+41	X'	Motor A transient reactance - pu	0.12
J+42	X"	Motor A subtransient reactance - pu	0.104
J+43	To'	Motor A transient open circuit time constant - s	0.095
J+44	To"	Motor A subtransient open circuit time constant - s	0.0021
J+45	H	Motor A inertia constant	0.1
J+46	etrq	Motor A exp for variation of torque with speed	0
J+47	Vtr1	Motor A 1st undervoltage trip voltage - pu	0.75
J+48	Ttr1	Motor A 1st undervoltage trip delay - s	0.06
J+49	Ftr1	Motor A 1st undervoltage trip fraction	0.1
J+50	Vrc1	Motor A 1st undervoltage reclose voltage - pu	0.8
J+51	Trc2	Motor A 1st undervoltage reclose delay - s	99999
J+52	Vtr2	Motor A 2nd undervoltage trip voltage - pu	0.62
J+53	Ttr2	Motor A 2nd undervoltage trip delay - s	0.021

CON	Parameters	Description	Value
J+54	Ftr2	Motor A 2nd undervoltage trip fraction	0.2
J+55	Vrc2	Motor A 2nd undervoltage reclose voltage - pu	0.7
J+56	Trc2	Motor A 2nd undervoltage reclose delay - s	0.1

Table 36 Motor B performance parameters

CON	Parameters	Description	Value
J+57	Mtyp	Motor B phase - always 3	3
J+58	LF	Motor B real power to power base ratio	0.75
J+59	Ra	Motor B stator resistance - pu on motor base	0.03
J+60	X	Motor B synchronous reactance - pu	1.8
J+61	X'	Motor B transient reactance - pu	0.19
J+62	X"	Motor B subtransient reactance - pu	0.14
J+63	To'	Motor B transient open circuit time constant - s	0.2
J+64	To"	Motor B subtransient open circuit time constant - s	0.0026
J+65	H	Motor B inertia constant	0.5
J+66	etrq	Motor B torque speed exponent	2
J+67	Vtr1	Motor B 1st undervoltage trip voltage - pu	0.7
J+68	Ttr1	Motor B 1st undervoltage trip delay - s	0.02
J+69	Ftr1	Motor B 1st undervoltage trip fraction	0.1
J+70	Vrc1	Motor B 1st undervoltage reclose voltage - pu	0.75
J+71	Trc2	Motor B 1st undervoltage reclose delay - s	0.05
J+72	Vtr2	Motor B 2nd undervoltage trip voltage - pu	0.45
J+73	Ttr2	Motor B 2nd undervoltage trip delay - s	0.021
J+74	Ftr2	Motor B 2nd undervoltage trip fraction	0.2
J+75	Vrc2	Motor B 2nd undervoltage reclose voltage - pu	0.6
J+76	Trc2	Motor B 2nd undervoltage reclose delay - s	0.05

Table 37 Motor C performance parameters

CON	Parameters	Description	Val
J+77	Mtyp	Motor C phase - always 3	3
J+78	LF	Motor C real power to power base ratio	0.75
J+79	Ra	Motor C stator resistance - pu on motor base	0.03
J+80	X	Motor C synchronous reactance - pu	1.8
J+81	X'	Motor C transient reactance - pu	0.19
J+82	X"	Motor C subtransient reactance - pu	0.14
J+83	To'	Motor C transient open circuit time constant - s	0.2
J+84	To"	Motor C subtransient open circuit time constant - s	0.0026
J+85	H	Motor C inertia constant	0.1
J+86	etrq	Motor C torque speed exponent	2
J+87	Vtr1	Motor C 1st undervoltage trip voltage - pu	0.8

CON	Parameters	Description	Val
J+88	Ttr1	Motor C 1st undervoltage trip delay - s	0.03
J+89	Ftr1	Motor C 1st undervoltage trip fraction	0.1
J+90	Vrc1	Motor C 1st undervoltage reclose voltage - pu	0.8
J+91	Trc1	Motor C 1st undervoltage reclose delay - s	9999
J+92	Vtr2	Motor C 2nd undervoltage trip voltage - pu	0.5
J+93	Ttr2	Motor C 2nd undervoltage trip delay - s	0.03
J+94	Ftr2	Motor C 2nd undervoltage trip fraction	0.2
J+95	Vrc2	Motor C 2nd undervoltage reclose voltage - pu	0.6
J+96	Trc2	Motor C 2nd undervoltage reclose delay - s	0.11

Table 38 Motor D performance parameters

CON	Parameters	Description	Value
J+97	Tstall	Motor D stall delay time - s	0.04
J+98	Trestart	Motor D restart from stall delay time - s	0.3
J+99	Tv	Motor D voltage time constant for contactors - s	0.025
J+100	Tf	Motor D frequency time constant for contactors - s	0.05
J+101	CompLF	Motor D real power to motor base ratio	1
J+102	CompPF	Motor D power factor at 1.0 pu voltage	1
J+103	Vstall	Motor D stall Voltage - pu	0.6
J+104	Rstall	Motor D stall resistance - pu of motor base	0.17
J+105	Xstall	Motor D stall reactance - pu of motor base	0.07
J+106	LFadj	Adjustment to stall voltage if COMPLF /= 1.0	0
J+107	Kp1	Motor D real power coeff when voltage > Vbrk	0
J+108	Np1	Motor D real power exp when voltage > Vbrk	1
J+109	Kq1	Motor D reactive power coeff when voltage > Vbrk	6
J+110	Nq1	Motor D reactive power exp when voltage>Vbrk	2
J+111	Kp2	Motor D real power coeff when voltage < Vbrk	12
J+112	Np2	Motor D real power exp when voltage < Vbrk	3.2
J+113	Kq2	Motor D reactive power coeff when voltage < Vbrk	11
J+114	Nq2	Motor D reactive power exp when voltage < Vbrk	2.5
J+115	Vbrk	Motor D "break-down" voltage	0.86
J+116	Frst	Motor D fraction capable of restart after stall	0.55
J+117	Vrst	Motor D voltage for restart after stall - pu	0.90
J+118	CmpKpf	Motor D real power frequency dependency	1
J+119	CmpKqf	Motor D reactive power freq dependency	-3.3
J+120	Vc1off	Motor D voltage contactors start opening - pu	0.5
J+121	Vc2off	Motor D voltage all contactors opened - pu	0.4
J+122	Vc1on	Motor D voltage all contactors closed - pu	0.6
J+123	Vc2on	Motor D voltage contactors start closing - pu	0.5
J+124	Tth	Motor D heating time constant - s	16

CON	Parameters	Description	Value
J+125	Th1t	Motor D temperature where tripping begins - pu	0.7
J+126	Th2t	Motor D temperature where completely tripped	1.9
J+127	Fuvr	Motor D fraction with undervoltage relays	0.1
J+128	UVtr1	Motor D 1st undervoltage pick-up - pu	0.6
J+129	Ttr1	Motor D 1st undervoltage trip delay - s	0.02
J+130	UVtr2	Motor D 2nd undervoltage pick-up - pu	0
J+131	Ttr2	Motor D 2nd under voltage trip delay - s	9999

A5. CMLD version 1 and version 2 comparison

This appendix provides a comparison between the CMLD version 1 and CMLD version 2 parameters for two cases:

1. An actual power system event for which there are high-speed monitoring (HSM) measurements available (8 March 2018). This event provides a comparison of the model transient behaviour with real measured data. However, the depth of the fault is not sufficient to lead to Motor D stall behaviour, and therefore does not illustrate the differences between the two model versions. At the time of this report, no historical actual events were available with measured data and a sufficiently low voltage dip to lead to Motor D stall behaviour.
2. A hypothetical event. This allows comparison of the transient behaviours of the two models in response to a deeper (credible) fault that does lead to Motor D stall behaviour. However, no actual measurements are available for comparison with the model outcomes.

A5.1.1 Actual power system event (8 March 2018)

On 8 March 2018, the Loy Yang Power Station B1 generator tripped due to an explosion/fire at the generator transformer. More details on this event can be found in the original CMLD and DER model report published in 2022[32] . Figure 15 shows the voltage, active power and reactive power at two key nodes: Loy Yang 500kV (location of the fault) and Bendigo 22kV terminal stations. The transient response of the version 1 and version 2 CMLD models is similar. The voltage at most buses remains above the threshold where Motor D stall behaviour would be observed, so the updates to the Motor D parameters in the CMLD model do not lead to a significant difference between the two model versions.

Figure 15 CMLD version 1 vs CMLD version 2 during the modelled event on 8/3/18

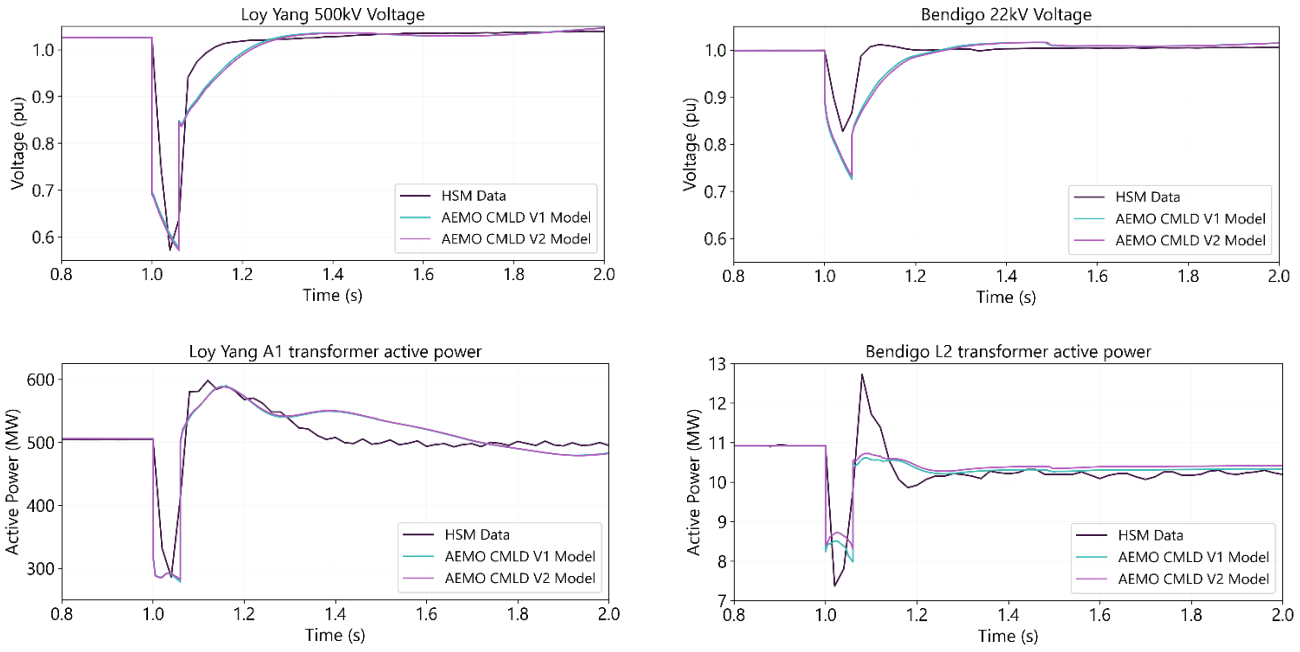

[32] Section 5.1, at https://aemo.com.au/-/media/files/initiatives/der/2022/psse-models-for-load-and-distributed-pv-in-the-nem.pdf?la=en

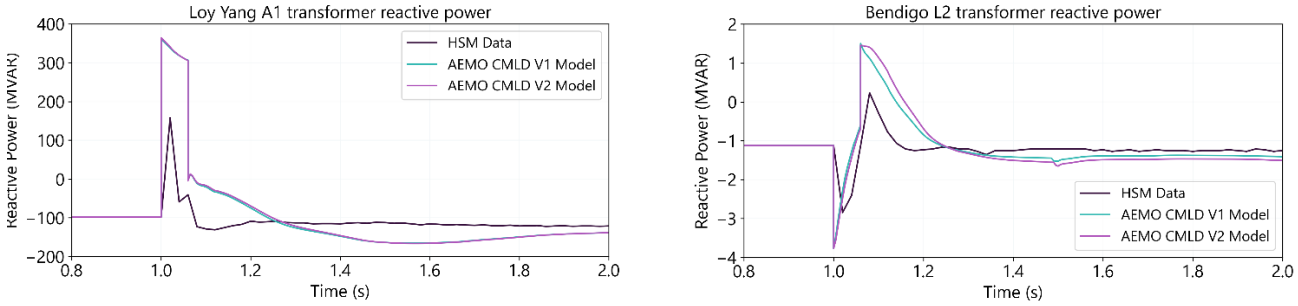

A5.1.2 Hypothetical event

To further explore the differences between the two versions of the CMLD models, a hypothetical case used in the VNI limit investigation (as outlined in Section 2.4) was studied. This case modelled a 2 phase to ground fault and trip of Hazelwood-South Morang 500 kV line 2 in a randomly selected night-time snapshot (19th September 2023 at 5:00am). This contingency is used to define the VNI export transient stability limit as outlined in the Victorian transfer limit advice report[33]. This fault results in a deeper voltage depression, so the response of the CMLD model under more onerous network conditions can be studied.

Figure 16 shows the voltage response of both the CMLD version 1 and CMLD version 2 model at Hazelwood 500kV (location of the fault) and Bendigo 22kV terminal stations, and the total underlying load response in Victoria. There is a more noticeable difference between the model versions in this case. This deeper fault stalls Motor D in the CMLD model, which is the component of the model designed to replicate Fault Induced Delayed Voltage Recovery (FIDVR) (refer to Section 2.1.1). The differences between the version 1 and version 2 CMLD parameters (detailed in Section 2) mean that the dynamics caused by FIDVR are less severe in the version 2 response. This results in a smaller impact to the transient stability limits.

Figure 16 CMLD version 1 vs CMLD version 2 during Hazelwood-South Morang 2PH-G fault

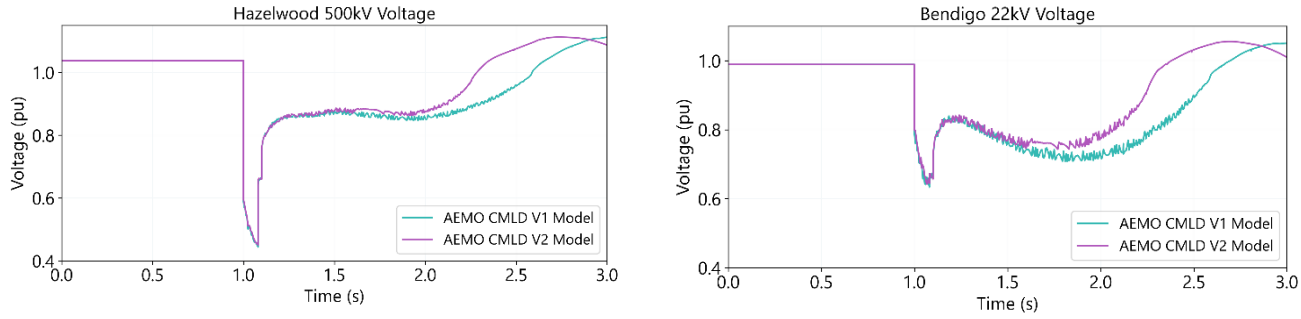

[33] Section 2, at https://www.aemo.com.au/-/media/files/electricity/nem/security_and_reliability/congestion-information/2024/victorian-transfer-limit-advice-system-normal_v28.pdf?la=en

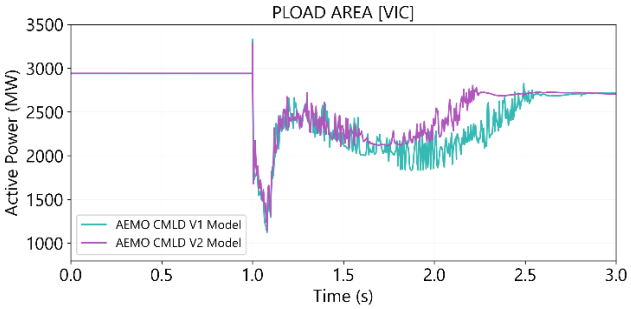

Note: PLOAD AREA [VIC] is a proxy for total underlying load in Victoria. This channel is set up using a channel subsystem (pssy.chsb()) API command in PSSE to measure the power totals across Victoria.

Figure 17 shows the difference in flows across the VIC-NSW cutset.

Figure 17 CMLD version 1 vs CMLD version 2 during Hazelwood-South Morang1PH-G fault: impact to Vic-NSW flows

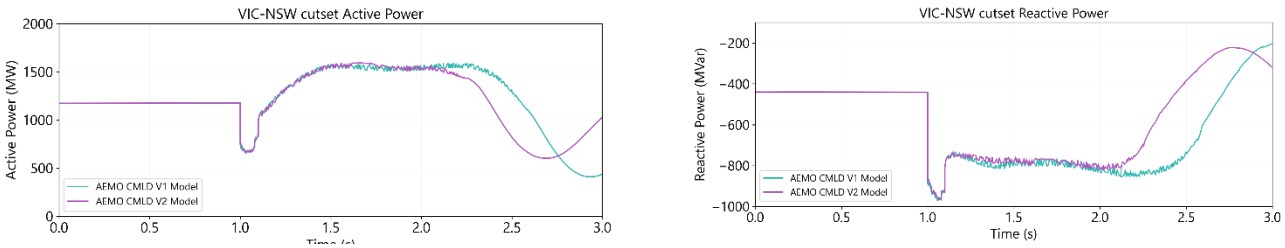

Until recently, there hasn't been a real event that has caused a deep transmission fault throughout the network to validate FIDVR behaviours in the CMLD model.

However, on 13th February 2024, the Moorabool (MLTS) – Sydenham (SYTS) No. 1 and 2 500 kilovolt (kV) lines tripped following the failure of six 500 kV towers[34]. This event is under investigation at present for preparation of an incident report, and might be suitable for use in validating the CMLD and DPV model dynamics in the future.

[34] AEMO (February 2024) Preliminary Report – Trip of Moorabool – Sydenham 500 kV No. 1 and No. 2 lines on 13 February 2024, at https://aemo.com.au/-/media/files/electricity/nem/market_notices_and_events/power_system_incident_reports/2024/preliminary-report---loss-of-moorabool---sydenham-500-kv-lines-on-13-feb-2024.pdf?la=en

A6. Transient behaviour validation testing

This appendix provides further detail on the SLIB testing of the CMLD and DERAEMO1 models against observations for a series of deep voltage disturbances in the Victorian network, where high speed monitoring is available at radial load locations. Further discussion and a summary of these results is provided in Section 3.2.3.

A6.1 25/07/2022

	Details
Incident report	Incident Report
Lowest measured voltage	0.63 pu at Red Cliffs Terminal Station (RCTS)
Event description	Failed bushing at Buronga resulting in a 220 kV phase to ground fault.
Event sequence	Simultaneous trip of: RCTS – Buronga 220 kV transmission line (0X1) Buronga – Broken Hill 220 kV transmission line (X2) at the Buronga end only Buronga – Balranald 220 kV transmission line (X3) at both ends. Buronga Synchronous Condenser No. 1, No. 2 and No. 3
HSM available	Red Cliffs Terminal Station (RCTS) – 0.63pu
PSS®E modelling approach	Using playback model to replicate measured voltage and frequency traces from HSM data, as described in Section 3.2.2.

Figure 18 Red Cliffs (RCTS)

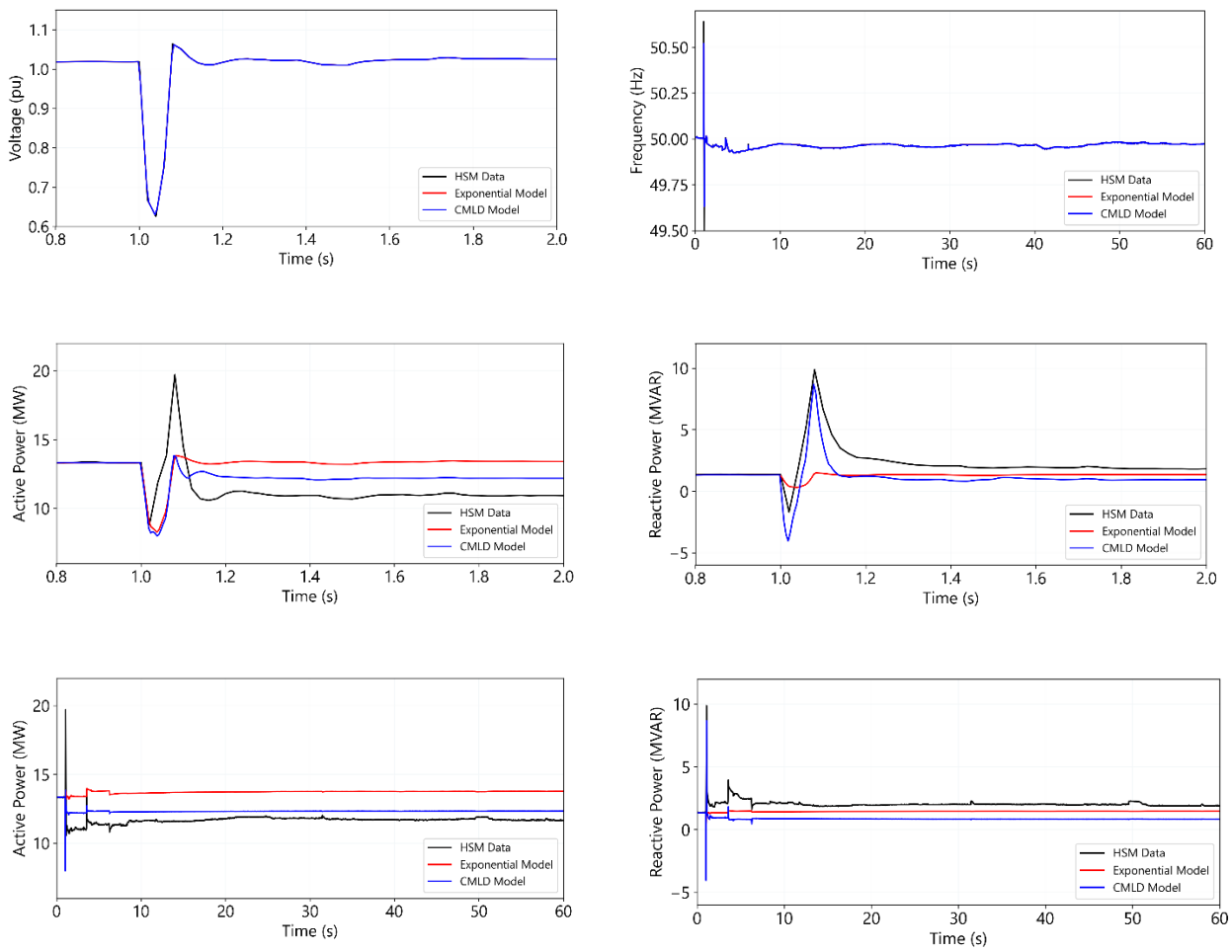

A6.2 18/01/2018

	Details
Incident report link	Incident report
Lowest measured voltage	0.64pu at Cranbourne Terminal Station (CBTS)
Event description	Failed 500 kV current transformer (CT) associated with the A2 transformer at ROTS.
Event sequence	Simultaneous trip of: Rowville No. 2 500kV busbar A2 500/220kV Transformer ROTS-SMTS 500 kV line at SMTS side only.
HSM available	Brooklyn (BLTS) – 0.82pu Cranbourne (CBTS) – 0.64 pu Rowville (ROTS) / Springvale (SVTS) – 0.68pu Templestowe (TSTS) – 0.70 pu

	Details
PSS®E modelling approach	Using playback model to replicate measured voltage and frequency traces from HSM data, as described in Section 3.2.2.

Figure 19 Brooklyn (BLTS)

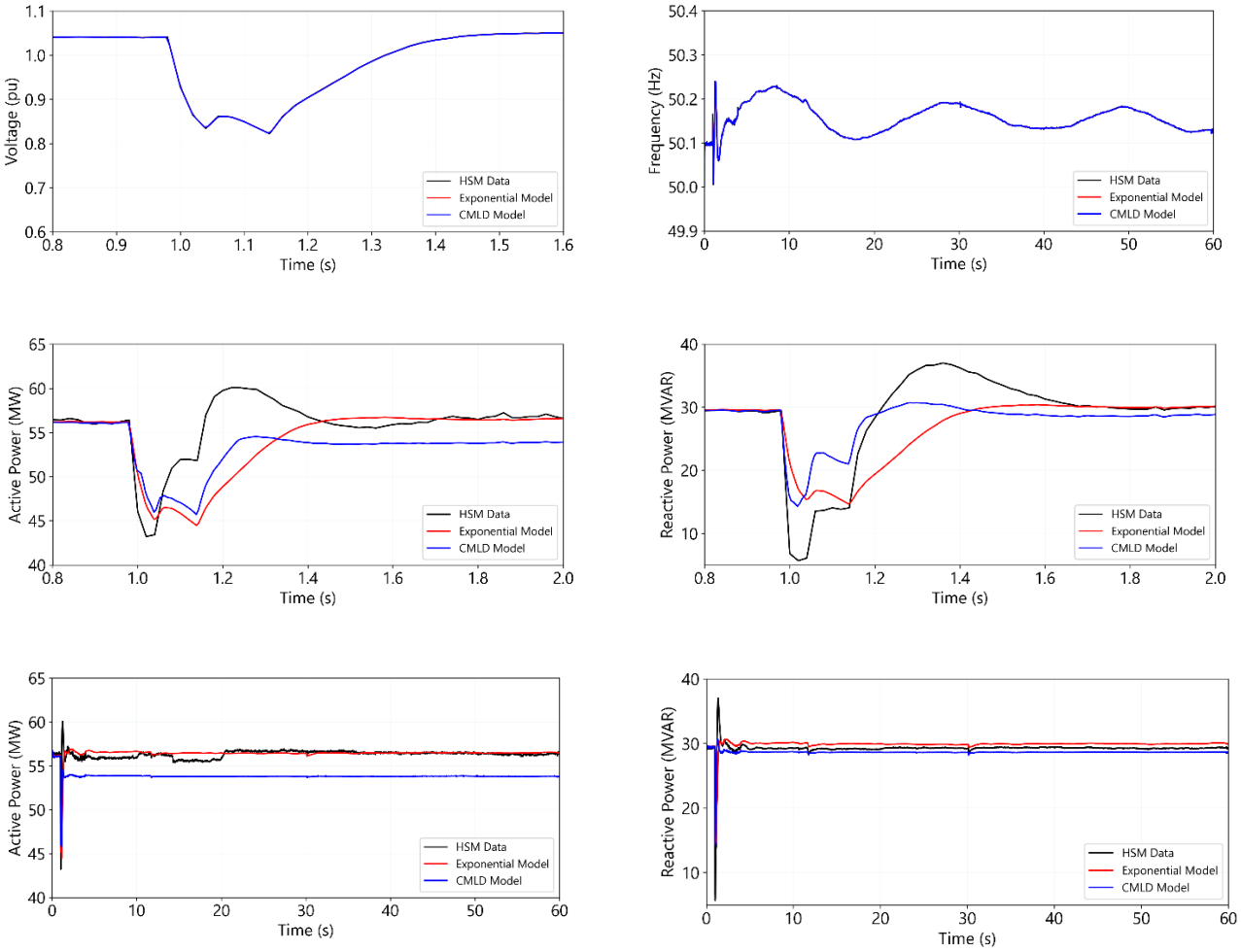

Figure 20 Cranbourne (CBTS)

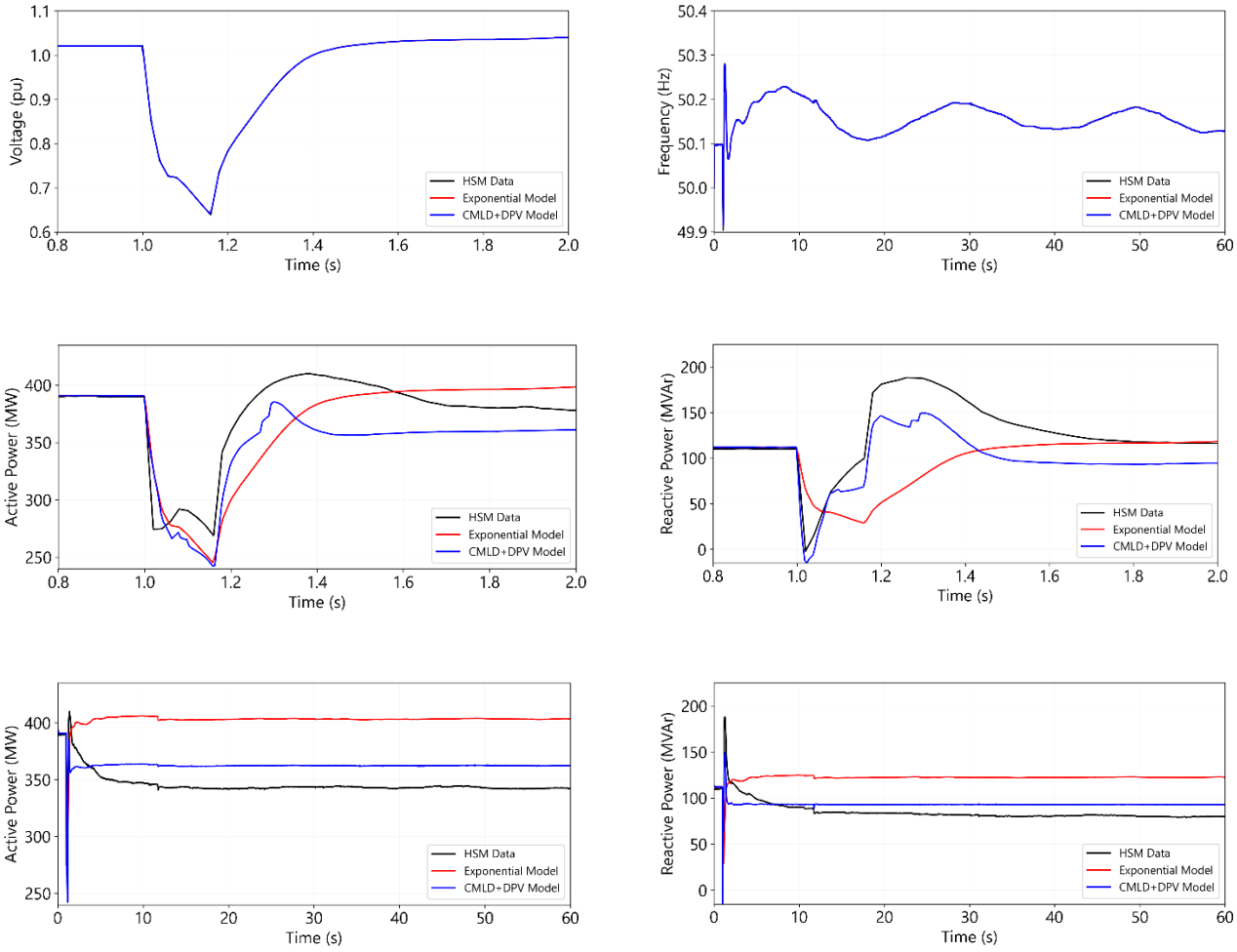

Figure 21 Rowville (ROTS) / Springvale (SVTS)

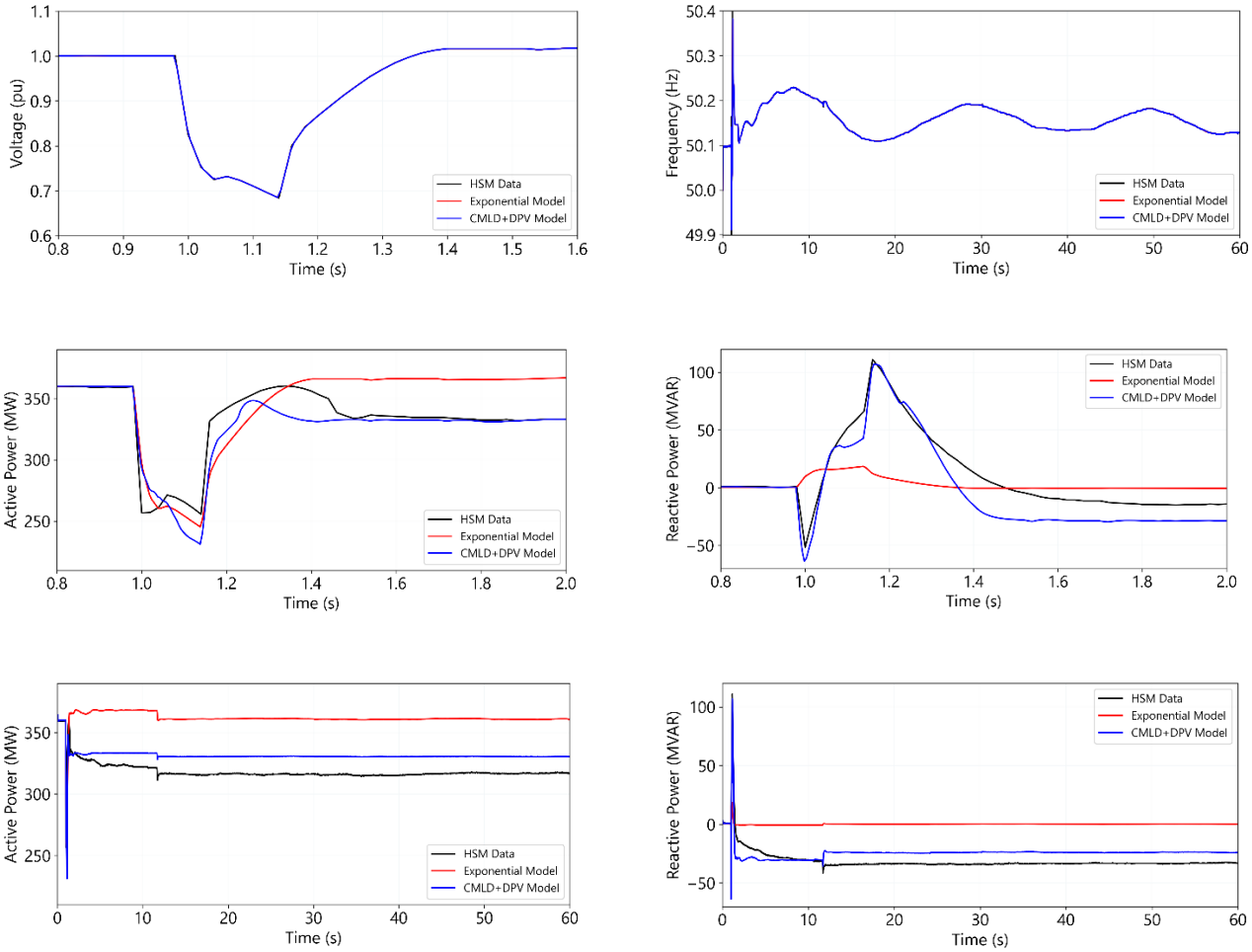

Figure 22 Templestowe (TSTS)

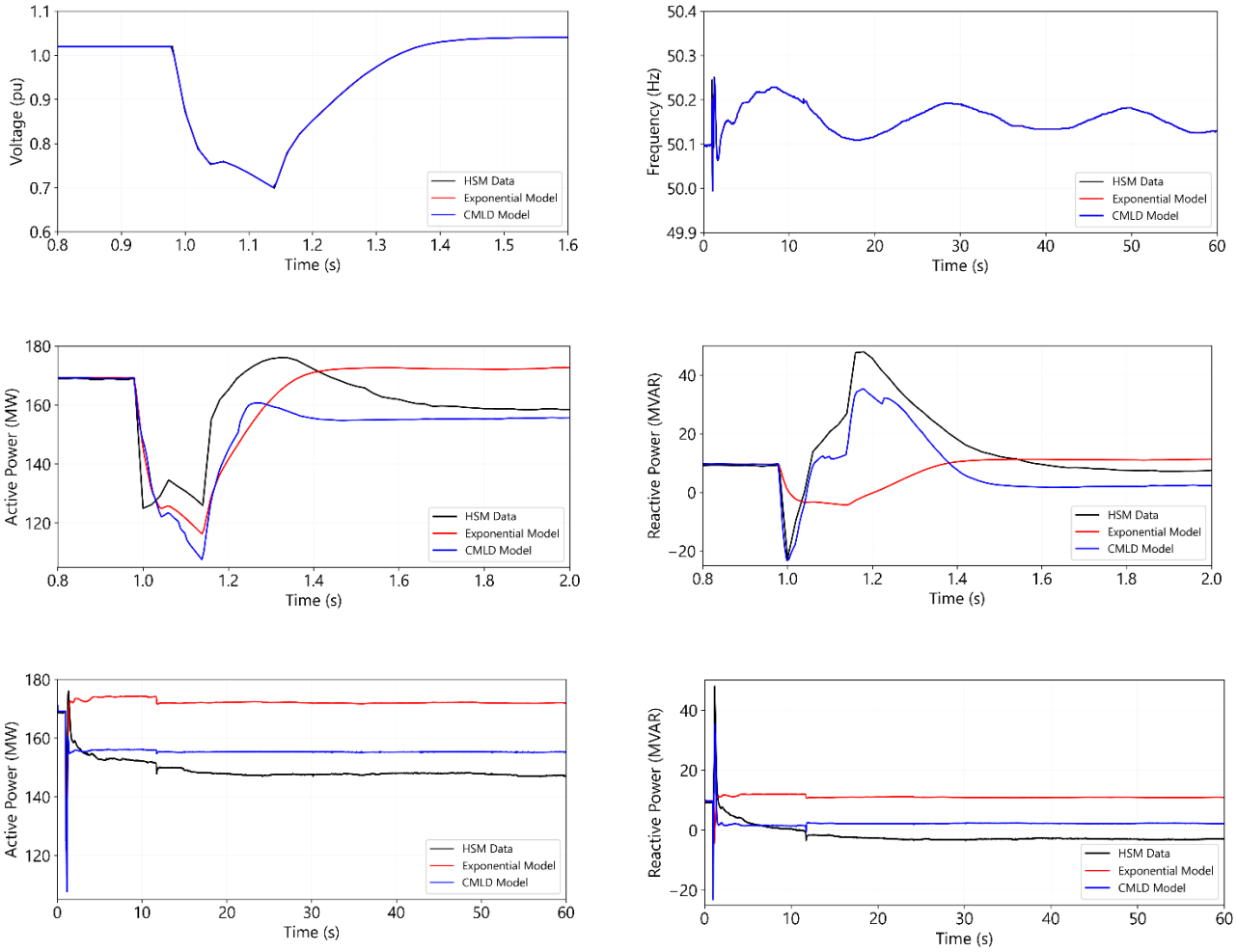

A6.3 31/01/2020

	Details
Incident report link	Incident Report
Lowest measured voltage	0.74pu at Brooklyn Terminal Station (BLTS)
Event description	Major weather event led to the collapse of several steel transmission towers on the MLTS-MOPS and MLTS-HGTS 500 kV lines, resulting in a Victoria and South Australia separation event.
Event sequence	Simultaneous trip of: MLTS-MOPS 500 kV line MLTS-HGTS 500 kV line HGTS-TGTS 500 kV line.
HSM available	Brooklyn (BLTS) – 0.74pu Cranbourne (CBTS) – 0.76pu Rowville (ROTS) / Springvale (SVTS) – 0.76pu Templestowe (TSTS) – 0.77pu

	Details
PSS®E modelling approach	Using playback model to replicate measured voltage and frequency traces from HSM data, as described in Section 3.2.2.

Figure 23 Brooklyn (BLTS)

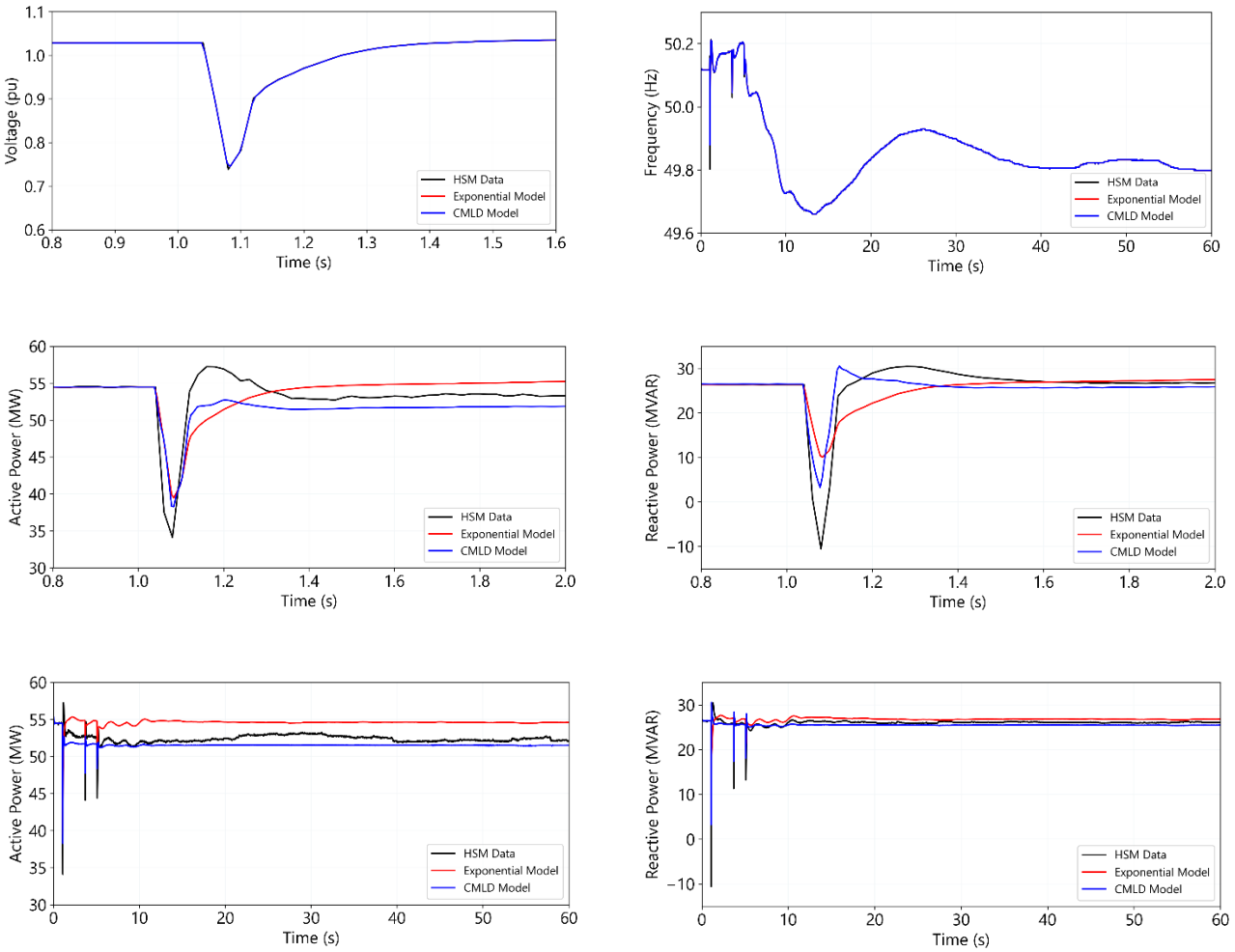

Figure 24 Cranbourne (CBTS)

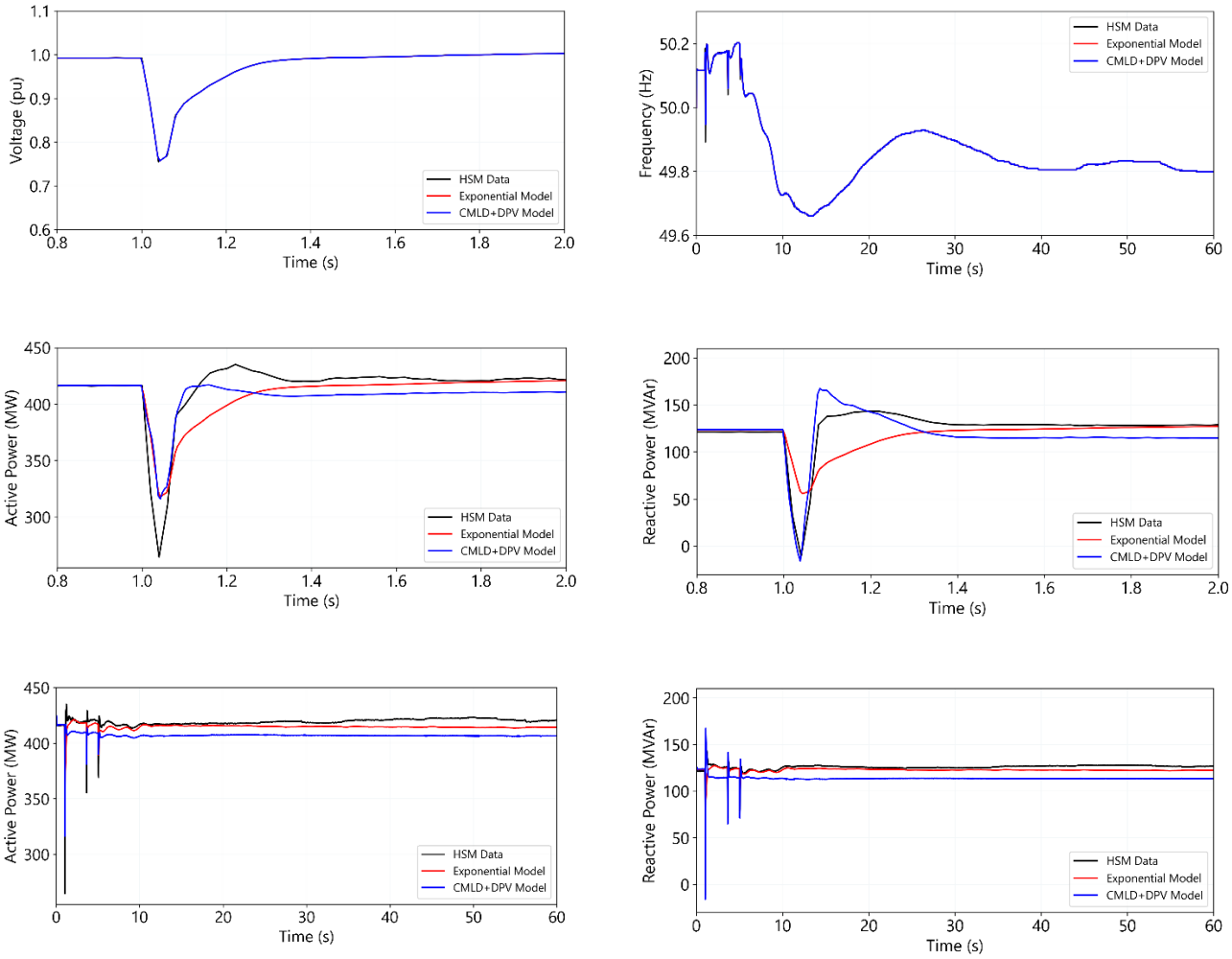

Figure 25 Rowville (ROTS) / Springvale (SVTS)

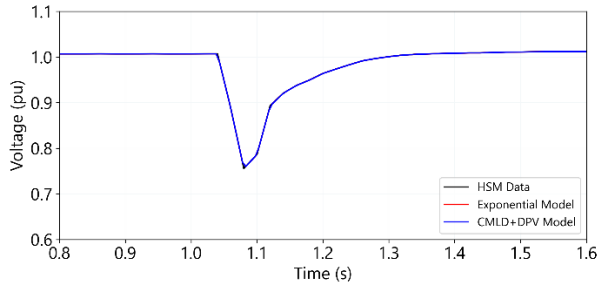

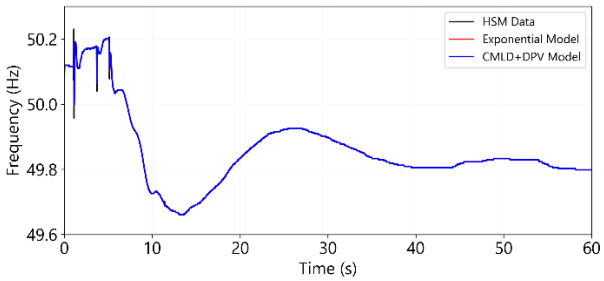

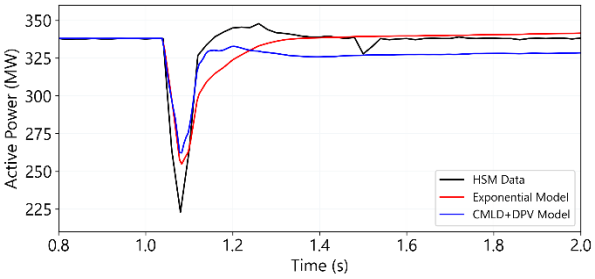

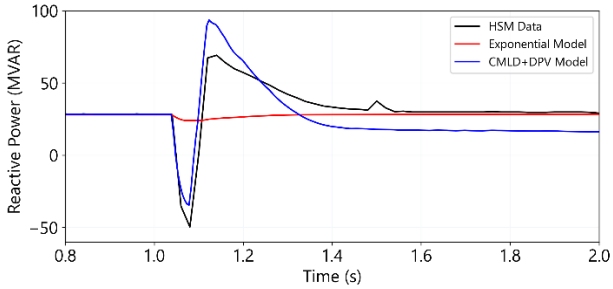

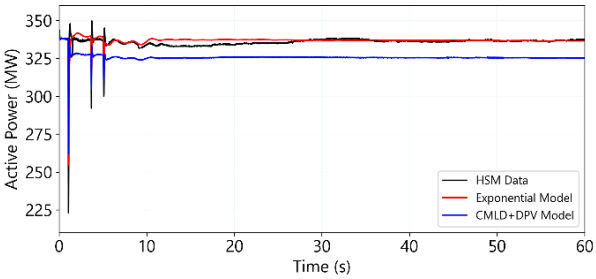

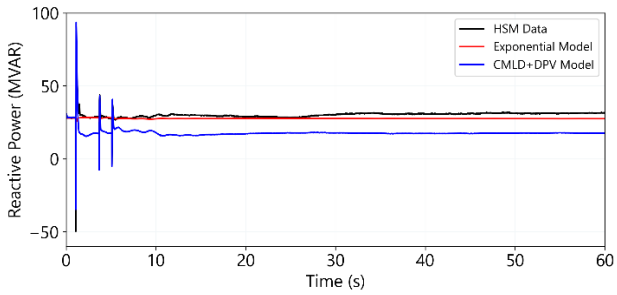

Figure 26 Templestowe (TSTS)

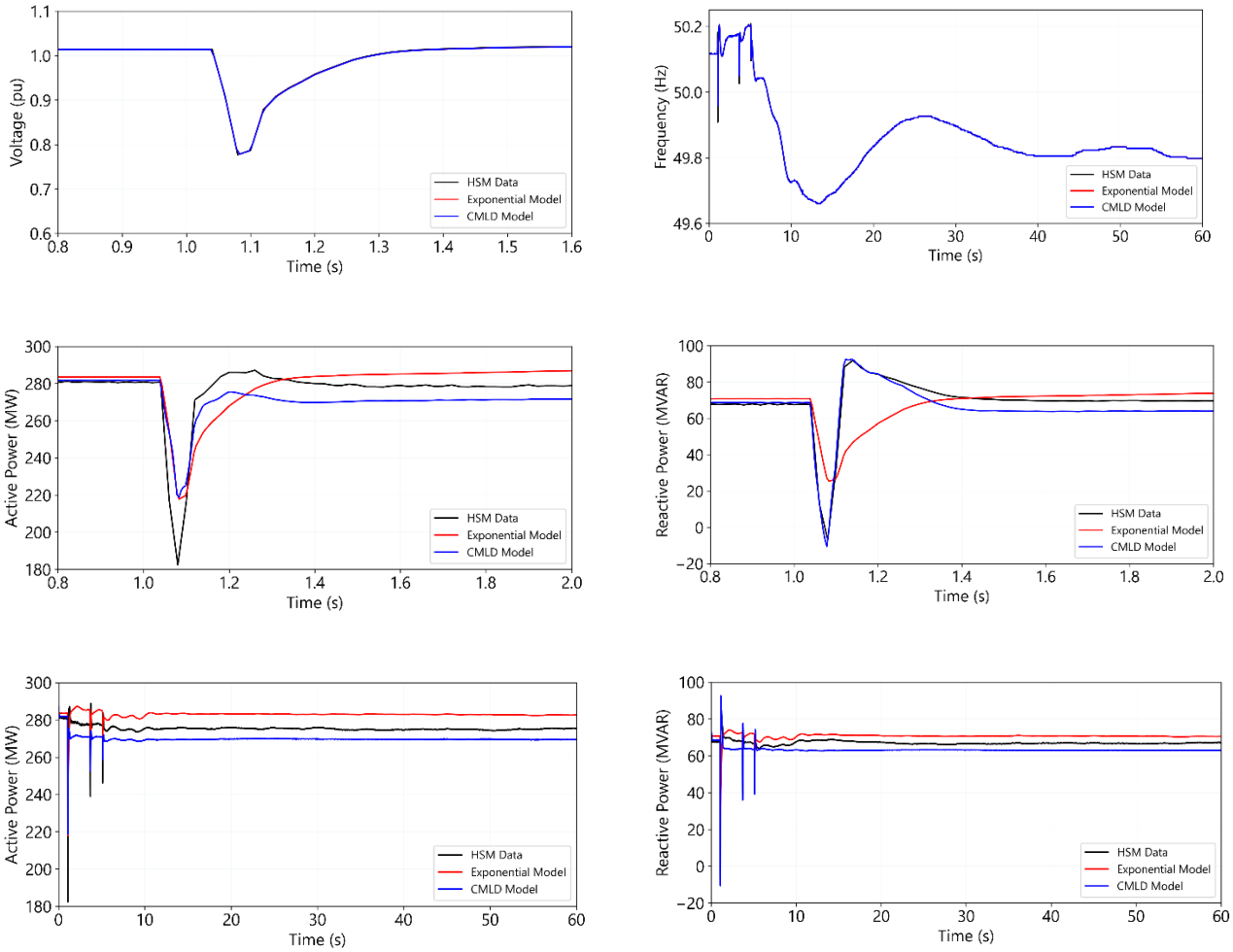

A6.4 8/03/2018

	Details
Lowest measured voltage	0.75pu at Rowville (ROTS) / Springvale (SVTS)
Details	Explosion/fire at Loy Yang 500/20 kV transformer leads to the trip of Loy Yang B1 unit.
Event sequence	LYB1 generator trip.
HSM available	Rowville (ROTS) / Springvale (SVTS) – 0.75pu Templestowe (TSTS) – 0.77pu
PSS®E modelling approach	Using playback model to replicate measured voltage and frequency traces from HSM data, as described in Section 3.2.2.

Figure 27 Rowville (ROTS) / Springvale (SVTS)

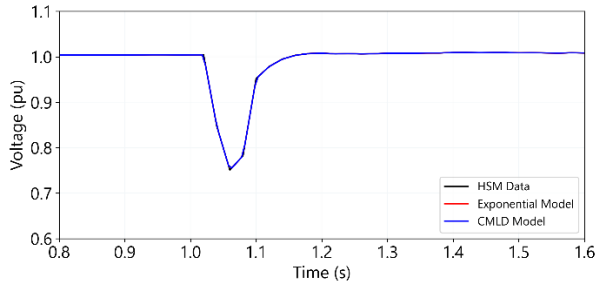

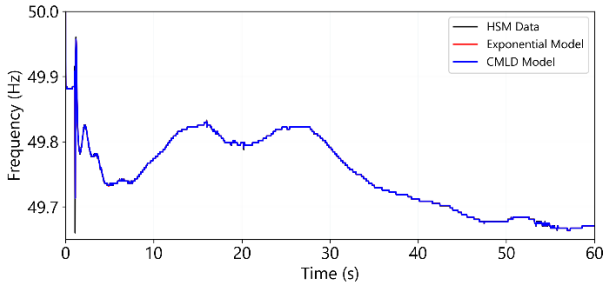

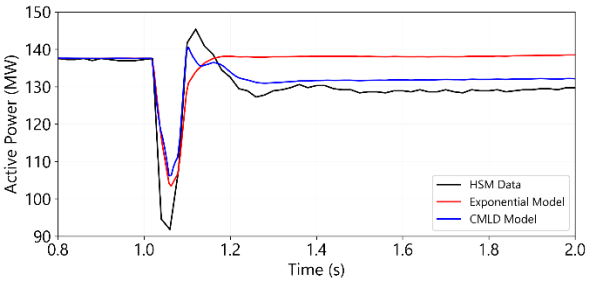

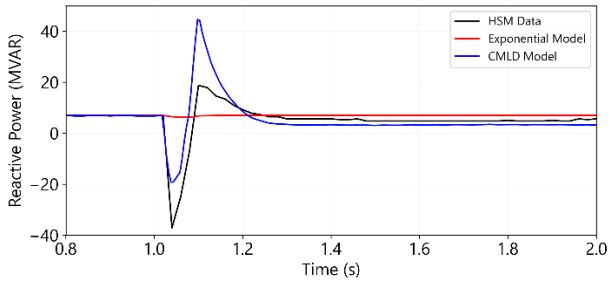

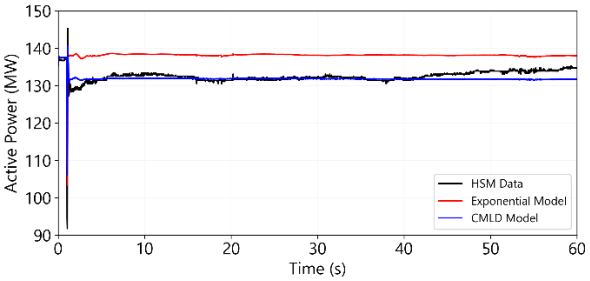

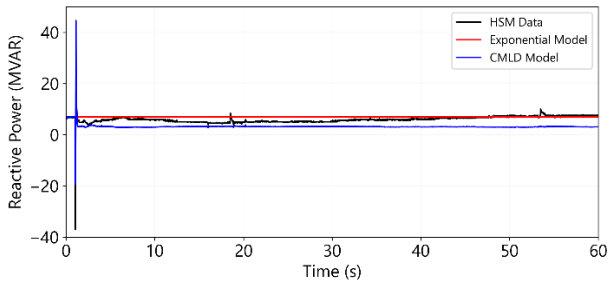

Figure 28 Templestowe (TSTS)

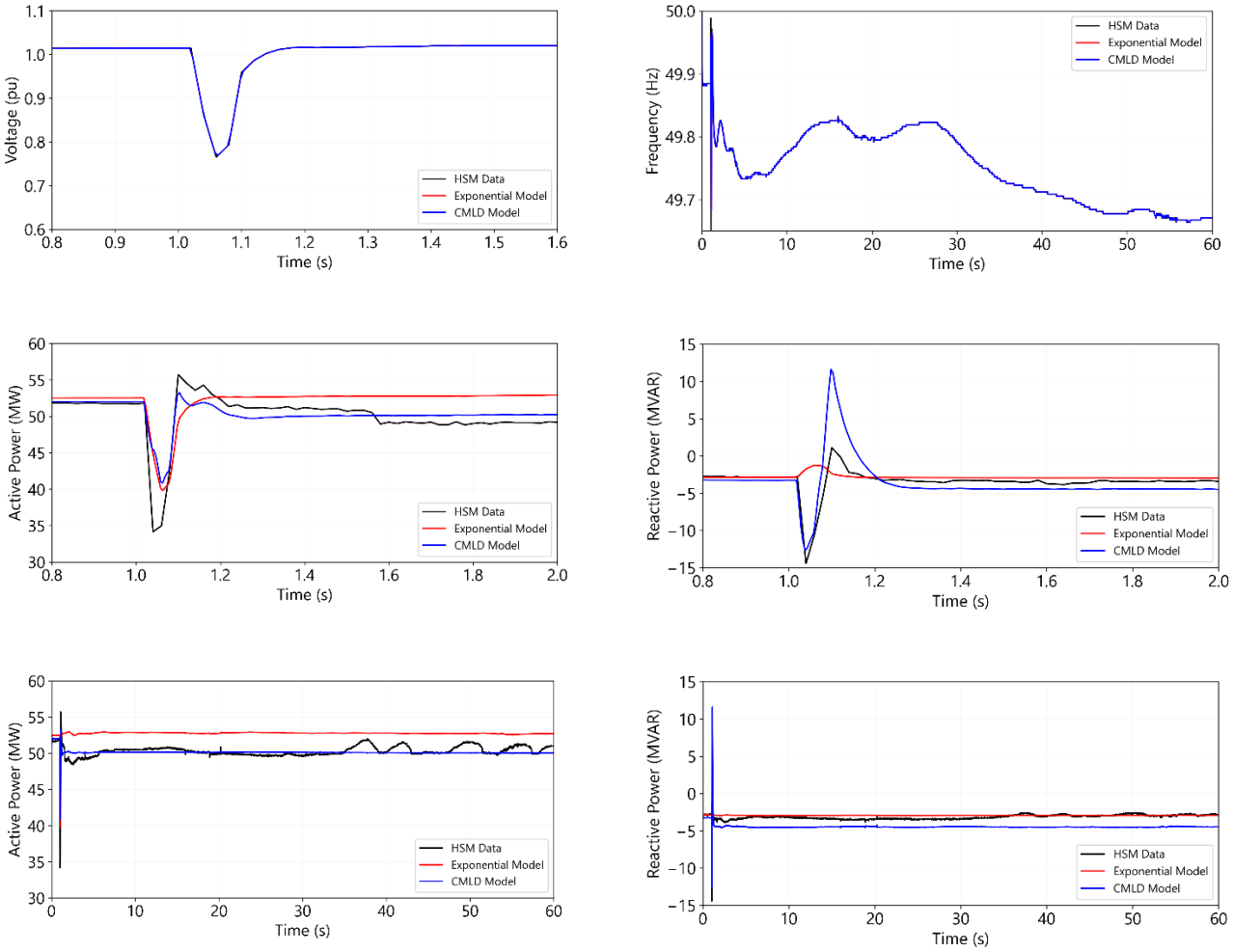

A6.5 18/02/2019

	Table text
Incident report link	Incident report
Lowest measured voltage	0.84pu at Rowville (ROTS) / Springvale (SVTS)
Event description	A phase to ground fault led to the trip of the Sydenham-Moorabool No. 2 500kV line and the Sydenham-Keilor 500kV line.
Event sequence	Simultaneous trip of: SYTS-MLTS 500 kV 2 line SYTS-KTS 500 kV line. This led to the outage of SYTS No 2 500kV busbar.
HSM available	Rowville (ROTS) / Springvale (SVTS) – 0.84pu
PSS®E modelling approach	Using playback model to replicate measured voltage and frequency traces from HSM data, as described in Section 3.2.2.

Figure 29 Rowville (ROTS) / Springvale (SVTS)

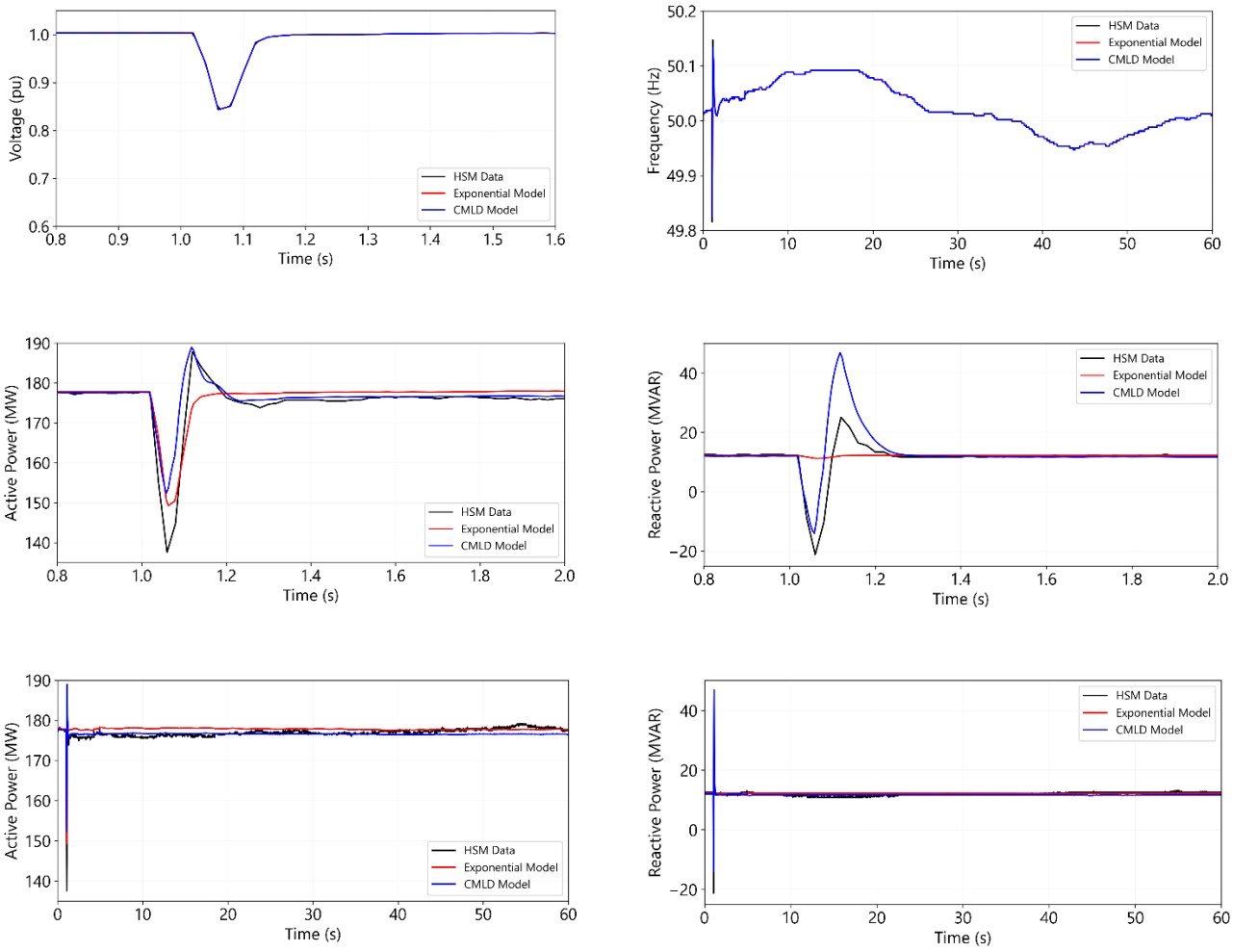

A7. Motor D composition estimates

This Appendix provides further detail on the approach for estimating the seasonal proportions of Motor D load. An estimate of the total Motor D load was calculated by multiplying:

- The estimated number of Motor D units operating by
- The estimated power consumption per unit

with both factors varying by season and day/night.

A7.1 Estimating the number of residential AC units operating

The 2021 Residential Baseline Study[35] (RBS) provides estimates of the stock of all residential appliances for all of Australia. The 2023 stocks of AC ducted and AC non-ducted were taken from Table 22 of that study.

The RBS dataset does not provide a breakdown of appliances into those that are single-phase induction motor driven, versus those that are inverter driven (and therefore should not be represented in the Motor D category). To estimate this proportion, an estimate from the EES report[36] was applied (Figure 33, estimated stock of inverter driven air conditioners in Australia by year). It was estimated that in 2023, ~5% of residential ACs in Australia are single-phase motor driven. The same proportion was applied for both ducted and non-ducted ACs.

The CSIRO study[37] provides an estimate of the relationship between AC usage on a given day versus the ambient temperature (also accounting for the difference between the maximum temperature of a given day and the previous day). The average temperature for each seasonal interval in each region was used to select a designated temperature curve[38], and the average value used to determine an approximate proportion of AC units online in that interval, in each region.

A7.2 Estimating power consumption per unit

Average seasonal estimates

Seasonal day/night estimates of power consumption by ducted and non-ducted AC units were estimated based on the CSIRO study[39]. This study monitored power consumption for a sample of individual residential AC units in Brisbane, Melbourne and Adelaide during 2012 to 2017. Estimated individual unit load profiles from the EES

[35] Australian Government (11 November 2022) 2021 Residential Baseline Study for Australia and New Zealand for 2000 to 2040, https://www.energyrating.gov.au/industry-information/publications/report-2021-residential-baseline-study-australia-and-new-zealand-2000-2040

[36] Energy Efficient Strategies (31 July 2020) Single Phase Induction Motor Loads on the NEM from Refrigeration and Air Conditioners, https://aemo.com.au/-/media/files/initiatives/der/2020/2020-08-05-ees-ac-load-composition.pdf?la=en

[37] M..Goldsworthy, CSIRO, (24 August 2017). "Towards a Residential Air-Conditioner Usage Model for Australia", https://www.mdpi.com/1996-1073/10/9/1256

[38] Figure 7, Probability of a/c usage on the given day versus the difference between the given days maximum apparent ambient temperature and the maximum apparent temperature on the preceding day for different values of today's maximum apparent temperature.

[39] M..Goldsworthy, CSIRO, (24 August 2017). "Towards a Residential Air-Conditioner Usage Model for Australia", https://www.mdpi.com/1996-1073/10/9/1256

report[40] were also used (Figures 37 to 42). Non-ducted AC power consumption per unit was determined from wall split AC load profiles. Monthly traces were averaged into seasonal periods.

For non-ducted AC units, a scaling factor was used to convert power consumption per ducted AC unit to that of a non-ducted AC unit (comparing the peaks of the average ducted and non-ducted AC load profiles from Figures 37 to 42 in the EES report). Since NSW was not included in the CSIRO study, VIC load profiles and hourly graphs were used as a proxy for the power consumption per unit for NSW.

Peak summer estimates

For estimating power consumption per unit for the peak summer periods, Figures 44 to 46 from the EES report were used. These figures show the hourly variation in the power consumption of a ducted AC unit for different cities. The peak summer power consumption per unit ducted AC was selected to be the maximum power consumed.

Conversion from inverter based to motor driven AC units

It is assumed that majority of the AC units monitored in the CSIRO study are inverter based. As a result of this, the power consumption per unit determined from the load profiles are likely more representative of an inverter driven unit rather than a motor driven unit. A 1.44 scaling factor was applied to the power per unit obtained from the CSIRO load profiles to convert the inverter-based power consumption per unit to a motor-based value. This scaling factor was sourced from an air conditioner power consumption study[41] which indicated a 44% increase in power consumption for motor driven ACs vs inverter driven ACs when monitoring the power consumption of inverter and non-inverter AC units over a 108-day period.

[40] Energy Efficient Strategies (31 July 2020) Single Phase Induction Motor Loads on the NEM from Refrigeration and Air Conditioners, https://aemo.com.au/-/media/files/initiatives/der/2020/2020-08-05-ees-ac-load-composition.pdf?la=en

[41] Almogbel et al. (7 December 2020) “Comparison of energy consumption between non-inverter and inverter-type air conditioner in Saudi Arabia”, https://link.springer.com/article/10.1007/s41825-020-00033-y#:~:text=The%20cooling%20period%20in%20Jeddah,AC's%20is%206230%20KWh%2Fyear